

On Convex Data-Driven Inverse Optimal Control for Nonlinear, Non-stationary and Stochastic Systems ¹

Emiland Garrabe ^a, Hozefa Jesawada ^b, Carmen Del Vecchio ^b, Giovanni Russo ^a

^a*Department of Information and Electrical Engineering and Applied Mathematics, University of Salerno, Italy*

^b*Department of Engineering, University of Sannio, Benevento, Italy*

Abstract

This paper is concerned with a finite-horizon inverse control problem, which has the goal of reconstructing, from observations, the possibly non-convex and non-stationary cost driving the actions of an agent. In this context, we present a result enabling cost reconstruction by solving an optimization problem that is convex even when the agent cost is not and when the underlying dynamics is nonlinear, non-stationary and stochastic. To obtain this result, we also study a finite-horizon forward control problem that has randomized policies as decision variables. We turn our findings into algorithmic procedures and show the effectiveness of our approach via in-silico and hardware validations. All experiments confirm the effectiveness of our approach.

1 Introduction

Inverse optimal control/reinforcement learning (IOC/IRL) refer to the problem of reconstructing the cost driving the actions of an agent from input/output observations Ab Azar et al. (2020). Tackling IOC/IRL problems is crucial to many scientific domains from engineering, psychology, economics, management and computer science. However, a key challenge is that the underlying optimization can become ill-posed even for a linear deterministic dynamics with convex cost. Motivated by this, in a finite-horizon setting, we propose an algorithm enabling cost reconstruction via convex optimization. The underlying optimization problem is convex even when the agent cost is not and when the underlying dynamics is nonlinear, non-stationary and stochastic. The approach leverages probabilistic descriptions that can be obtained directly from data and/or from first-principles. We briefly survey some works related to the results/framework of this paper. For a comprehensive review on IOC/IRL we refer to Ab Azar et al. (2020).

Related Works. IOC methods were originally developed to determine control *functions* that generate ob-

served outputs Bryson (1996). More recently, also driven by the advancements in computational power and the increase in the availability of data, there has been a renewed interest in IOC (and IRL) methods. For stationary Markov Decision Processes (MDPs) an approach based on maximum entropy is proposed in Ziebart et al. (2008), with the resulting algorithm based on a backward/forward pass scheme. The framework of maximum causal entropy is extended to the infinite time horizon setting in Zhou et al. (2018), where two formulations are proposed together with convex approximations. Additionally, following this research stream, Mehr et al. (2023) considers linear multi-agent games, while Levine and Koltun (2012) obtains results based on the local approximation of the cost/reward. Furthermore, Levine et al. (2011) also proposes a complementary approach based on the use of Gaussian Processes to model stochastic dynamics. The resulting algorithm requires matrix inversions and relies on optimization problems that are not convex in general. For stationary MDPS, Finn et al. (2016) builds on maximum-entropy and uses deep neural networks to estimate the cost. The approach is benchmarked on manipulation tasks. Also for manipulation tasks, Kalakrishnan et al. (2013) considers deterministic nonlinear systems, utilizing path integrals to learn the cost. In the context of deterministic systems, Self et al. (2022) introduces a model-based IRL algorithm, while Lian et al. (2022) tackles the IRL problem for multi-player non-cooperative games. Linearly solvable MDPs are exploited in Dvijotham and Todorov (2010) and within this framework one can obtain a convex optimization problem to estimate the cost. However, this

Email addresses: egarrabe@unisa.it (Emiland Garrabe), jesawada@unisannio.it (Hozefa Jesawada), c.delvecchio@unisannio.it (Carmen Del Vecchio), giovarusso@unisa.it (Giovanni Russo).

¹ An early version of this paper with a sketch of the proof for one of the results can be found in Garrabé et al. (2023). EG/HJ are joint first authors. Corresponding author: GR.

approach assumes that the agent can specify the state transition. A risk-sensitive IRL algorithm is proposed in Ratliff and Mazumdar (2020) for cost estimates in stationary MDPs assuming that the expert policy belongs to the exponential distribution. For LTI deterministic systems, in Xue et al. (2022) an IRL algorithm is presented that learns the parameters of a quadratic cost for tracking problems. In the context of IOC, Nakano (2023) considers stochastic dynamics and proposes an approach to estimate the parameters of a control regularizer for finite-horizon problems. For finite-horizon discrete-time linear quadratic regulators, in Yu et al. (2021) the cost parameters are estimated from noisy measurements. Also, Rodrigues (2022) tackles an IOC problem for known nonlinear deterministic systems with quadratic cost in the input. In Do (2019) infinite-horizon IOC problems are considered for inverse optimal stabilization and inverse optimal gain assignment for stochastic nonlinear systems driven by Lévy processes. In Deng and Krstić (1997), stabilization problems in an infinite-horizon setting are considered and it is shown that for every system with a stochastic control Lyapunov function, one can construct a controller which is optimal with respect to some cost. In Jouini and Rantzer (2022) the cost design problem is considered and combinations of input/states compatible with a given value function are studied. Finally, the approach we propose relies on a technical result to find the optimal solution for a related finite-horizon forward control problem. This problem has randomized policies as decision variables and and it is related to the problems considered in Kárný (1996); Todorov (2009); Kárný and Guy (2006) and references therein. See Garrabe and Russo (2022) for a survey on this class of sequential decision-making problems.

1.1 Contributions

We propose an inverse control algorithm, which enables cost reconstruction by solving an optimization problem that is convex even when the agent cost is not convex, non-stationary and when the dynamics is nonlinear, non-stationary and stochastic. To the best of our knowledge, this is the first algorithm featuring an underlying optimization problem that is guaranteed to be convex in this setting and that, at the same time: (i) does not require that the agent can specify its state transitions; (ii) does not assume a stationary/discounted setting; (iii) does not require solving forward problems in each iteration and can be used for stochastic systems. Our key technical contributions are as follows:

- (1) In the finite-horizon setting, we introduce a result to recast the IOC problem into a convex optimization problem. We show that convexity is guaranteed even when the task cost is not convex and non-stationary. Moreover, the result, which leverages certain probabilistic descriptions that can be obtained directly from data, does not require as-

- sumptions on the underlying dynamics besides the standard Markov assumption;
- (2) To obtain our result on the inverse problem, we also study a related Forward Optimal Control (FOC) problem. For this finite-horizon problem with randomized policies as decision variables, we give an expression of the optimal policy, exploited to tackle our IOC problem. We discuss when this problem has a bounded cost (for the precise definition see Assumption 1) and this also leads to a comprehensive discussion, interesting *per se*, relating the problem we consider to other control problem formulations that involve KL Divergence minimization;
- (3) The results for the inverse and the forward control problems are turned into algorithmic procedures. Leveraging these algorithms, we illustrate the effectiveness of our results on problems that involve both continuous and discrete states and actions. Moreover, we compare our IOC result with two state-of-the-art algorithms in the literature. The experiments illustrate that our algorithm outperforms those from the literature achieving a lower discrepancy between real and reconstructed costs with significantly lower computation times. Code available at <https://tinyurl.com/46uccxsf>;
- (4) The algorithms are validated via a hardware test-bed (the documented code for the experiments is available at <https://tinyurl.com/46uccxsf>). Namely, we use our algorithms to reconstruct the cost of robots navigating in an environment with the goal of reaching a desired destination. We consider both an obstacle-free environment (Scenario 1) and an environment populated with obstacles (Scenario 2). The experimental results, which are obtained for both continuous and discrete variables, demonstrate the effectiveness of our approach. Moreover, the paper also includes a running example involving the swing-up of a pendulum. The example illustrates some of the key algorithmic details of our results (code also available at <https://tinyurl.com/46uccxsf>).

While our results are related to works on IRL and IOC that leverage maximum entropy and likelihood arguments² such as Ziebart et al. (2008); Dvijotham and Todorov (2010); Zhou et al. (2018), this work extends these in several ways. First, we do not necessarily require that the MDP is stationary as instead assumed in these papers. Second, we show that the underlying optimization problem that we obtain to reconstruct the cost is convex even when the dynamics is stochastic and the agent cost is not convex and non-stationary. In Ziebart et al. (2008) convexity is guaranteed only when the MDP is deterministic. In Zhou et al. (2018) a convex IRL formulation is obtained but this relies on an approximation

² Notably, the exponential policies arising from our FOC problem and exploited to tackle the IOC are also *assumed* in these works. This is further discussed throughout the paper

of the original problem. Instead, we do not rely on approximations to obtain convexity. Third, the approach we propose can be used for both continuous and discrete action/state spaces, while Ziebart et al. (2008); Dvijotham and Todorov (2010); Zhou et al. (2018) tackle IRL/IOC problems with discrete variables. Moreover, we do not require that the agent is able to specify its state transitions as instead assumed in Dvijotham and Todorov (2010). Additionally, in Ziebart et al. (2008); Zhou et al. (2018), policy evaluation is required at each iteration of the algorithm and this is not required with our approach. Finally, we also deploy the policies from the FOC problem on a setup involving real hardware. Consequently, we also show that the cost can be effectively reconstructed from these policies. This was not done in the above works.

2 Mathematical Background

Sets are in *calligraphic* and vectors in **bold**. We let \mathbb{K} be either \mathbb{R} or \mathbb{Z} . A random variable is denoted by \mathbf{V} and its realization is \mathbf{v} . We denote the *probability mass function* (pmf, for discrete variables) or *probability density function* (pdf, for continuous variables) of \mathbf{V} by $p(\mathbf{v})$ and we let \mathcal{D} be the convex subset of pdfs/pmfs. In what follows, we simply say that $p(\mathbf{v})$ is a probability function (pf). Whenever we take the sums/integrals involving pfs we always assume that they exist. The expectation of a function $\mathbf{h}(\cdot)$ of a discrete \mathbf{V} is denoted $\mathbb{E}_p[\mathbf{h}(\mathbf{V})] := \sum_{\mathbf{v}} \mathbf{h}(\mathbf{v})p(\mathbf{v})$, where the sum is over the support of $p(\mathbf{v})$; whenever it is clear from the context, we omit the subscript in the sum (for continuous variables the summation is replaced by the integral on the support of $p(\mathbf{v})$). The joint pf of \mathbf{V}_1 and \mathbf{V}_2 is denoted by $p(\mathbf{v}_1, \mathbf{v}_2)$ and the conditional pf of \mathbf{V}_1 with respect to (w.r.t.) \mathbf{V}_2 is $p(\mathbf{v}_1 | \mathbf{v}_2)$. Countable sets are denoted by $\{w_k\}_{k_1:k_n}$, where w_k is the generic set element, k_1 (k_n) is the index of the first (last) element and $k_1 : k_n$ is the set of consecutive integers between (including) k_1 and k_n . A pf of the form $p(\mathbf{v}_0, \dots, \mathbf{v}_N)$ is compactly written as $p_{0:N}$ (by definition $p_{k:k} := p_k(\mathbf{v}_k)$). We compactly write conditional pfs of the form $p_k(\mathbf{y}_k | \mathbf{z}_{k-1})$ as $p_{k|k-1}^{(y)}$. Also, functionals are denoted by capital calligraphic characters with arguments within curly brackets. We make use of the Kullback-Leibler (KL, Kullback and Leibler (1951)) divergence, a measure of the proximity of the pair of pmfs $p(\mathbf{v})$ and $q(\mathbf{v})$, defined for discrete variables as $D_{\text{KL}}(p || q) := \sum_{\mathbf{v}} p(\mathbf{v}) \ln(p(\mathbf{v})/q(\mathbf{v}))$. For continuous variables the sum is replaced by the integral. The $D_{\text{KL}}(p || q)$ is finite only if the support of $p(\mathbf{v})$ is contained in the support of $q(\mathbf{v})$. That is, $D_{\text{KL}}(p || q)$ is finite only if $p(\mathbf{v})$ is absolutely continuous with respect to (w.r.t.) $q(\mathbf{v})$, see e.g., (Cover and Thomas, 2006, Chapter 8). We recall the chain rule for the KL divergence:

Lemma 1 *Let \mathbf{V} and \mathbf{Z} be two random variables and let $f(\mathbf{v}, \mathbf{z})$ and $g(\mathbf{v}, \mathbf{z})$ be two joint pfs. Then:*

$$D_{\text{KL}}(f(\mathbf{v}, \mathbf{z}) || g(\mathbf{v}, \mathbf{z})) = D_{\text{KL}}(f(\mathbf{v}) || g(\mathbf{v})) + \mathbb{E}_{f(\mathbf{v})}[D_{\text{KL}}(f(\mathbf{z} | \mathbf{v}) || g(\mathbf{z} | \mathbf{v}))].$$

2.1 Problems Set-up

We let $\mathbf{X}_k \in \mathcal{X} \subseteq \mathbb{K}^n$ be the system state at time-step k and $\mathbf{U}_k \in \mathcal{U} \subseteq \mathbb{K}^p$ be the control input at time-step k . The time indexing is chosen so that the system transitions to \mathbf{x}_k when \mathbf{u}_k is applied. That is, by making the Markov assumption, the possibly non-stationary, non-linear stochastic dynamics for the system under control is given by the pf $p_k^{(x)}(\mathbf{x}_k | \mathbf{u}_k, \mathbf{x}_{k-1})$. In what follows, we make use of the short-hand notation $p_{k|k-1}^{(x)}$ to denote this pf, which is simply termed as target pf.

Remark 1 *In the running example we obtain the target pf from data. We let $\Delta_k := (\mathbf{x}_{k-1}, \mathbf{u}_k)$ be a data pair. Also, $\Delta_{0:N} := (\{\Delta_k\}_{1:N}, \mathbf{x}_N)$ is the dataset collected over $\mathcal{T} := 0 : N$. A database is a collection of datasets.*

To formalize the control problems we introduce the pf:

$$p_{0:N} = p_0(\mathbf{x}_0) \prod_{k=1}^N p_{k|k-1} = p_0(\mathbf{x}_0) \prod_{k=1}^N p_{k|k-1}^{(x)} p_{k|k-1}^{(u)}, \quad (1)$$

where $p_{k|k-1}^{(u)} := p_k^{(u)}(\mathbf{u}_k | \mathbf{x}_{k-1})$ is a randomized policy and initial conditions are embedded via the prior $p_0(\mathbf{x}_0)$. Also, we use the shorthand notation $p_{k|k-1} := p_{k|k-1}^{(x)} p_{k|k-1}^{(u)} = p_k(\mathbf{x}_k, \mathbf{u}_k | \mathbf{x}_{k-1})$.

Remark 2 *At each k , the pf $p_k^{(x)}(\mathbf{x}_k | \mathbf{u}_k, \mathbf{x}_{k-1})$ describes the behavior of the system given \mathbf{x}_{k-1} and \mathbf{u}_k ; $p_{0:N}$ describes in probabilistic terms the evolution of closed-loop system when, at each k , a given policy, say $p_k^{(u)}(\mathbf{u}_k | \mathbf{x}_{k-1})$, is used. With the forward control problem (Section 2.2) we aim to design the policy. This is then exploited to tackle the inverse problem (Section 2.3).*

2.2 The Forward Control Problem

We let $c_k : \mathcal{X} \rightarrow \mathbb{R}$ be the cost, at time-step k , associated to \mathbf{x}_k . Then, the expected cost incurred when the system is in state \mathbf{x}_{k-1} and input \mathbf{u}_k is applied is given by $\mathbb{E}_{p_{k|k-1}^{(x)}}[c_k(\mathbf{X}_k)]$. The forward control problem considered in this paper is formalized with the following:

Problem 1 *Given a joint pf*

$$q_{0:N} := q_0(\mathbf{x}_0) \prod_{k=1}^N q_k^{(x)}(\mathbf{x}_k | \mathbf{u}_k, \mathbf{x}_{k-1}) q_k^{(u)}(\mathbf{u}_k | \mathbf{x}_{k-1}),$$

find the sequence of pfs, $\left\{p_{k|k-1}^{(u)\star}\right\}_{1:N}$, such that:

$$\begin{aligned} \left\{p_{k|k-1}^{(u)\star}\right\}_{1:N} \in \arg \min_{\left\{p_{k|k-1}^{(u)}\right\}_{1:N}} & \left\{ D_{KL}(p_{0:N} \parallel q_{0:N}) \right. \\ & \left. + \sum_{k=1}^N \mathbb{E}_{\bar{p}_{k-1:k}} \left[\mathbb{E}_{p_{k|k-1}^{(x)}} [c_k(\mathbf{X}_k)] \right] \right\} \quad (2) \\ \text{s.t. } p_{k|k-1}^{(u)} \in \mathcal{D} \quad & \forall k \in \mathcal{T}. \end{aligned}$$

where $\bar{p}_{k-1:k} := p_{k-1}(\mathbf{x}_{k-1}, \mathbf{u}_k)$.

The solution of Problem 1 is a sequence of randomized policies. At each k , the control input applied to the system, i.e. \mathbf{u}_k^* , is sampled from $p_{k|k-1}^{(u)\star}$.

Remark 3 In Problem 1, minimizing the first term in the cost functional amounts at minimizing the discrepancy between $p_{0:N}$ and $q_{0:N}$. Hence, this first term can be thought of as a regularizer, biasing the behaviour of the closed loop system towards $q_{0:N}$. In Remark 6 we discuss how the optimal solution of the problem changes when a regularization weight is introduced in the formulation.

Typically, $q_{0:N}$ can be a passive dynamics Cammardella et al. (2019); Todorov (2009) or capture behaviors from demonstrations Gagliardi and Russo (2022). The pfs for the dynamics in Problem 1 can be derived both directly from the data (see e.g., our running example) and from first-principles. This setting, which foresees randomized policies as decision variables, is widely adopted in the literature, see e.g. Cammardella et al. (2019); Kárný and Guy (2006); Guan et al. (2014); Todorov (2009) and Garrabe and Russo (2022) for a survey across learning and control. Moreover, as we shall see, the class of policies obtained as optimal solution of Problem 1 also naturally arises in the context of IOC/IRL, see e.g., Zhou et al. (2018); Todorov (2009); Ziebart et al. (2008). For this last point, see also Remark 7.

For our derivations, it is also useful to define $q_{k|k-1}^{(x)} := q_k^{(x)}(\mathbf{x}_k | \mathbf{u}_k, \mathbf{x}_{k-1})$, $q_{k|k-1}^{(u)} := q_k^{(u)}(\mathbf{u}_k | \mathbf{x}_{k-1})$ and $q_{k|k-1} := q_{k|k-1}^{(x)} q_{k|k-1}^{(u)} = q_k(\mathbf{x}_k, \mathbf{u}_k | \mathbf{x}_{k-1})$. When emphasizing the cost dependency on the decision variables in Problem 1, we use the notation $\mathcal{J} \left\{ p_{k|k-1}^{(u)} \right\}_{1:N}$.

Assumption 1 For Problem 1, there exists some feasible $\left\{ \tilde{p}_{k|k-1}^{(u)} \right\}_{1:N}$ such that $\mathcal{J} \left\{ \tilde{p}_{k|k-1}^{(u)} \right\}_{1:N}$ is bounded, that is, there exist some \underline{J} and \bar{J} such that $-\infty < \underline{J} \leq \mathcal{J} \left\{ \tilde{p}_{k|k-1}^{(u)} \right\}_{1:N} \leq \bar{J} < +\infty$.

We now discuss Assumption 1. To this aim, we define

$$\tilde{q}_{0:N} := \frac{q_{0:N} \exp \left(- \sum_{k=1}^N \tilde{c}_k(\mathbf{x}_{k-1}, \mathbf{u}_k) \right)}{\sum_{\mathbf{x}_{0:N}, \mathbf{u}_{1:N}} q_{0:N} \exp \left(- \sum_{k=1}^N \tilde{c}_k(\mathbf{x}_{k-1}, \mathbf{u}_k) \right)}, \quad (3)$$

with $\tilde{c}_k(\mathbf{x}_{k-1}, \mathbf{u}_k) := \mathbb{E}_{p_{k|k-1}^{(x)}} [c_k(\mathbf{X}_k)]$. By leveraging the Markov assumption, the above pf can be decomposed as

$$\tilde{q}_{0:N} := \tilde{q}_0(\mathbf{x}_0) \prod_{k=1}^N \tilde{q}_k^{(x)}(\mathbf{x}_k | \mathbf{u}_k, \mathbf{x}_{k-1}) \tilde{q}_k^{(u)}(\mathbf{u}_k | \mathbf{x}_{k-1}),$$

and again we use the shorthand notation $\tilde{q}_{k|k-1}^{(x)}$ and $\tilde{q}_{k|k-1}^{(u)}$ to denote $\tilde{q}_k^{(x)}(\mathbf{x}_k | \mathbf{u}_k, \mathbf{x}_{k-1})$ and $\tilde{q}_k^{(u)}(\mathbf{u}_k | \mathbf{x}_{k-1})$, respectively. Also, we let $\tilde{q}_{k|k-1} := \tilde{q}_{k|k-1}^{(x)} \tilde{q}_{k|k-1}^{(u)}$ and note that $\mathcal{J} \left\{ \tilde{p}_{k|k-1}^{(u)} \right\}_{1:N}$ can be written as

$$D_{KL}(p_{0:N} \parallel \tilde{q}_{0:N}) - \sum_{\mathbf{x}_{0:N}, \mathbf{u}_{1:N}} q_{0:N} \exp \left(- \sum_{k=1}^N \tilde{c}_k(\mathbf{x}_{k-1}, \mathbf{u}_k) \right). \quad (4)$$

Then, we are ready to give the following:

Proposition 1 Consider Problem 1 and assume that:

- (i) there exist non-negative constants $H_k < +\infty$, $k = 0 : N$ such that $D_{KL}(p_0(\mathbf{x}_0) \parallel \tilde{q}_0(\mathbf{x}_0)) \leq H_0$ and, $\forall k = 1 : N$, $D_{KL}(p_{k|k-1}^{(x)} \parallel \tilde{q}_{k|k-1}^{(x)}) \leq H_k$;
- (ii) there exist some \bar{e} such that

$$\mathbb{E}_{q_{0:N}} \left[\exp \left(- \sum_{k=1}^N \tilde{c}_k(\mathbf{x}_{k-1}, \mathbf{u}_k) \right) \right] \leq \bar{e} < +\infty.$$

Then, Assumption 1 is satisfied with $\left\{ \tilde{p}_{k|k-1}^{(u)} \right\}_{1:N} = \left\{ \tilde{q}_{k|k-1}^{(u)} \right\}_{1:N}$ and with $\underline{J} = -\bar{e}$ and $\bar{J} = \sum_{k=0}^N H_k$.

PROOF. See the appendix.

Remark 4 In Proposition 1, condition (i) is satisfied when $p_0(\mathbf{x}_0)$ and $p_{k|k-1}^{(x)}$ are absolutely continuous w.r.t. $\tilde{q}_0(\mathbf{x}_0)$ and $\tilde{q}_{k|k-1}^{(x)}$, respectively. Condition (ii) is satisfied whenever the agent cost $c_k(\cdot)$ is lower bounded.

Remark 5 From the above discussion, the problem in (1) has the same minimizer (but different optimal cost) as the problem $\min_{\left\{ p_{k|k-1}^{(u)} \right\}_{1:N}} D_{KL}(p_{0:N} \parallel \tilde{q}_{0:N})$. These cost functionals are also considered in the literature

on probabilistic design Kárný and Guy (2006), entropically regularized optimal transport Nutz (2020) and Shroedinger Bridges Chen et al. (2021).

2.3 The Inverse Control Problem

The inverse control problem we consider consists in recovering the cost-to-go for the agent, say $\bar{c}_k(\cdot)$, and the agent cost $c_k(\cdot)$ given a set of observed states and inputs sampled from $p_{k|k-1}^{(x)}$ and from the agent policy. In what follows, we denote by $\hat{\mathbf{x}}_k$ and $\hat{\mathbf{u}}_k$ the observed state and control input at time-step k . We also make the following:

Assumption 2 *The cost-to-go is expressed as a linear combination of features. That is, $\bar{c}_k(\mathbf{x}_k) = -\mathbf{w}_k^T \mathbf{h}(\mathbf{x}_k)$, where $\mathbf{h}(\mathbf{x}_k) := [h_1(\mathbf{x}_k), \dots, h_F(\mathbf{x}_k)]^T$ is the features vector and $h_i : \mathcal{X} \rightarrow \mathbb{R}$ are known functions, $i \in 1 : F$, and $\mathbf{w}_k := [w_{k,1}, \dots, w_{k,F}]^T$ is a vector of weights.*

The assumption is rather common in the literature see e.g., Ziebart et al. (2008); Mehr et al. (2023); Kalakrishnan et al. (2013); Self et al. (2022); Dvijotham and Todorov (2010). With our results in Section 3.2 we propose an approach based on maximum likelihood to recover $\bar{c}_k(\cdot)$ and $c_k(\cdot)$. See e.g., Yin et al. (2023) for a maximum likelihood framework for linear systems in the context of data-driven control.

Running Example: Pendulum Control

We consider the control of a pendulum and in this first part of the running example we introduce the setting³. The forward control problem consists in stabilizing a pendulum on its unstable equilibrium. The cost used to formulate this forward control problem (tackled in the next part of the example) is:

$$c(\mathbf{x}_k) = (\theta_k - \theta_d)^2 + 0.01(\omega_k - \omega_d)^2, \quad (5)$$

with $\theta_d = 0$ and $\omega_d = 0$ ($\theta_d = 0$ corresponds to the unstable equilibrium of the pendulum). With the inverse control problem, tackled in the last part of this running example, we recover the cost from observed states and control inputs.

The pendulum dynamics, which is only used to generate data, is given by:

$$\begin{aligned} \theta_k &= \theta_{k-1} + \omega_{k-1} dt + W_\theta \\ \omega_k &= \omega_{k-1} + \left(\frac{g}{l} \sin(\theta_{k-1}) + \frac{u_k}{ml^2} \right) dt + W_\omega, \end{aligned} \quad (6)$$

where θ_k is the angular position, ω_k is the angular velocity and u_k is the torque applied on the hinged end. The

³ All results were obtained using a laptop with an 12th Gen Intel Core i5-12500H 2.50 GHz processor and 18 GB of RAM

parameter l is the rod length, m is the mass of the pendulum, g is the gravity and $dt = 0.1s$ is the discretization step. Also, W_θ and W_ω are sampled from Gaussians, i.e. $W_\theta \sim \mathcal{N}(0, 0.05)$ and $W_\omega \sim \mathcal{N}(0, 0.1)$. We let $\mathbf{X}_k := [\theta_k, \omega_k]^T$ and $u_k \in \mathcal{U}$ with $\mathcal{U} := [-2.5, 2.5]$. The parameters were chosen as in Garrabe and Russo (2022) so that the target pendulum, i.e. the pendulum that we want to control, had parameters $m = 1\text{kg}$, $l = 0.6\text{m}$, while the reference pendulum (from which the pfs $q_{k|k-1}^{(x)}$ and $q_{k|k-1}^{(u)}$ are extracted) had $m = 0.5\text{kg}$, $l = 0.5\text{m}$. To illustrate the application of our results in both the continuous and the discrete settings, we built both pdfs and pmfs for the target and reference pendulum. These were built from data obtained by simulating (6). The process we followed is outlined below (see <https://tinyurl.com/46uccxsf> for the details).

Target pendulum. For the discrete setting, we estimated the empirical pmf, $p_{k|k-1}^{(x)}$, for the target pendulum. To do so, we set $\mathcal{X} := [-\pi, \pi] \times [-5, 5]$ and: (i) built a database of 10000 simulations of 100 time-steps each (at each step of the simulations the control input was sampled from the uniform distribution); (ii) discretized the set \mathcal{X} in 50×50 bins; (iii) used the histogram filter to estimate the empirical pmf from the data. The algorithm for the histogram filter can be found in e.g., Garrabe and Russo (2022) that also provides the related documented code. Instead, for the continuous setting we estimated the pdf $p_{k|k-1}^{(x)}$ via Gaussian Processes. To this aim, we: (i) used a database of 30 simulations and 100 time-steps to build a prior (again, at each k the control input was sampled from the uniform distribution); (ii) picked the covariance function as a squared exponential kernel. By doing so, at each k , $p_{k|k-1}^{(x)}$ was a Gaussian with mean and variance inferred from the data.

Reference pendulum. We estimated both a continuous and a discrete $q_{k|k-1}^{(x)}$ and this was done by following the process described above for the target pendulum. Instead, $q_{k|k-1}^{(u)}$ was obtained as in Garrabe and Russo (2022) by adding Gaussian noise to a Model Predictive Control (MPC) policy (able to stabilize the unstable equilibrium of the reference pendulum) and subsequently discretizing this pf.

3 Main Results

We first present a result tackling the forward control problem by giving the optimal solution of Problem 1. Then, this result is used to address the inverse control problem. To streamline the presentation, results are stated for discrete variables. The proofs for continuous variables are omitted here for brevity.

3.1 Tackling the Forward Control Problem

With the next result we give the solution to Problem 1.

Theorem 1 Consider Problem 1 and let Assumption 1 hold. Then:

(i) the problem has the unique solution $\{p_{k|k-1}^{(u)*}\}_{1:N}$, with

$$p_{k|k-1}^{(u)*} = \frac{\bar{p}_{k|k-1}^{(u)} \exp\left(-\mathbb{E}_{p_{k|k-1}^{(x)}}[\bar{c}_k(\mathbf{X}_k)]\right)}{\sum_{\mathbf{u}_k} \bar{p}_{k|k-1}^{(u)} \exp\left(-\mathbb{E}_{p_{k|k-1}^{(x)}}[\bar{c}_k(\mathbf{X}_k)]\right)}, \quad (7)$$

where

$$\bar{p}_{k|k-1}^{(u)} := q_{k|k-1}^{(u)} \exp\left(-D_{KL}\left(p_{k|k-1}^{(x)} \parallel q_{k|k-1}^{(x)}\right)\right), \quad (8)$$

where $\bar{c}_k : \mathcal{X} \rightarrow \mathbb{R}$ is given by

$$\bar{c}_k(\mathbf{x}_k) = c_k(\mathbf{x}_k) - \hat{c}_k(\mathbf{x}_k), \quad (9a)$$

with $\hat{c}_k : \mathcal{X} \rightarrow \mathbb{R}$ obtained via the backward recursion

$$\begin{aligned} \hat{c}_N(\mathbf{x}_N) &= 0, \\ \hat{c}_k(\mathbf{x}_k) &= \ln\left(\mathbb{E}_{q_{k+1|k}^{(u)}}\left[\exp\left(-D_{KL}\left(p_{k+1|k}^{(x)} \parallel q_{k+1|k}^{(x)}\right)\right.\right.\right. \\ &\quad \left.\left.\left.-\mathbb{E}_{p_{k+1|k}^{(x)}}[\bar{c}_{k+1}(\mathbf{X}_{k+1})]\right)\right]\right), \quad k = 1 : N-1; \end{aligned} \quad (9b)$$

(ii) the minimum is $-\sum_{k=1}^N \mathbb{E}_{\bar{p}_{k-1}}[\hat{c}_{k-1}(\mathbf{X}_{k-1})]$, where $\bar{p}_{k-1} := p_{k-1}(\mathbf{x}_{k-1})$.

Remark 6 It is often convenient to include in the formulation of the problem in (2) a regularization weight, say $\varepsilon > 0$, for the KL divergence component of the cost. In this case, the problem in (2) becomes

$$\begin{aligned} \left\{p_{k|k-1}^{(u)*}\right\}_{1:N} \in \arg \min & \left\{ \varepsilon D_{KL}(p_{0:N} \parallel q_{0:N}) \right. \\ & \left. + \sum_{k=1}^N \mathbb{E}_{\bar{p}_{k-1:k}} \left[\mathbb{E}_{p_{k|k-1}^{(x)}} [c_k(\mathbf{X}_k)] \right] \right\} \\ \text{s.t. } p_{k|k-1}^{(u)} & \in \mathcal{D} \quad \forall k \in \mathcal{T}. \end{aligned} \quad (10)$$

The optimal solution of (10) is again given by Theorem 1 with the only difference being in (9a) which now becomes $\bar{c}_k(\mathbf{x}_k) = c_k^{(\varepsilon)}(\mathbf{x}_k) - \hat{c}_k(\mathbf{x}_k)$, with $c_k^{(\varepsilon)}(\mathbf{X}_k) := c_k(\mathbf{X}_k)/\varepsilon$.

PROOF. The proof, which is by induction, is based on the steps of Gagliardi and Russo (2022); Russo (2021). In

Gagliardi and Russo (2022) the control problem had no $c_k(\cdot)$ while in Russo (2021) the cost was included, however the decision variables were not randomized policies. We give a self-contained proof in the appendix.

Remark 7 The optimal solution in Theorem 1 has an exponential twisted kernel Guan et al. (2014) and this structure is exploited to prove our result on the inverse problem. This class of policies, also known as softmax/Boltzmann policies, are often assumed in IRL/IOC works. For example, the policies in Ratliff and Mazumdar (2020); Ziebart et al. (2008); Zhou et al. (2018) can be derived from (7) and (8) when $q_{k|k-1}^{(u)}$ is uniform and $p_{k|k-1}^{(x)}$ is equal to $q_{k|k-1}^{(x)}$. The policy from which the agent cost is reconstructed in these works is in fact a softmax.

Remark 8 In Problem 1 the space of the policies is unconstrained. However, from (7) and (8) we get that the optimal solution given in Theorem 1 is zero whenever $q_{k|k-1}^{(u)} = 0$. That is, $q_{k|k-1}^{(u)}$ can be used to enforce that the optimal solution is zero for specific \mathbf{u}_k 's. In turn, this can be useful when \mathbf{u}_k has bound constraints.

3.1.1 Turning Theorem 1 into an Algorithm

Theorem 1 can be turned into an algorithmic procedure with steps given in Algorithm 1. The algorithm, which takes as input \mathcal{T} , $q_{0:N}$, $p_{k|k-1}^{(x)}$ and $c_k(\cdot)$ and outputs $\{p_{k|k-1}^{(u)*}\}_{1:N}$, computes $p_{k|k-1}^{(u)*}$ following (7) and (9).

Algorithm 1 Pseudo-code from Theorem 1: forward control algorithm

Inputs: \mathcal{T} , $q_{0:N}$, $p_{k|k-1}^{(x)}$ and $c_k(\cdot)$

Output: $\{p_{k|k-1}^{(u)*}\}_{1:N}$

for $k = N$ to 1 **do**

 Compute $\hat{c}_k(\mathbf{x}_k)$ using (9)

$\bar{c}_k(\mathbf{x}_k) \leftarrow c_k(\mathbf{x}_k) - \hat{c}_k(\mathbf{x}_k)$

 Compute $\bar{p}_{k|k-1}^{(u)}$ using (8)

$$p_{k|k-1}^{(u)*} \leftarrow \frac{\bar{p}_{k|k-1}^{(u)} \exp\left(-\mathbb{E}_{p_{k|k-1}^{(x)}}[\bar{c}_k(\mathbf{X}_k)]\right)}{\sum_{\mathbf{u}_k} \bar{p}_{k|k-1}^{(u)} \exp\left(-\mathbb{E}_{p_{k|k-1}^{(x)}}[\bar{c}_k(\mathbf{X}_k)]\right)}$$

end for

Remark 9 For continuous variables, the statement of Theorem 1 remains unchanged with the key difference being in the fact that computing the KL-divergence and expectations requires, in general, integrations (and not summations). As a result, while the steps shown in Algorithm 1 remain unchanged when the pfs are continuous, the integrals need to be estimated and this in general can be computationally difficult. Next, we discuss a case where the policy can be efficiently computed.

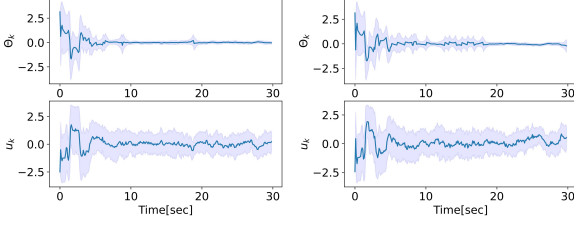


Fig. 1. Target pendulum angular position and corresponding control input. Results obtained when: (i) pfs are discrete, estimated via the histogram filter (left panels); (ii) pfs are estimated via Gaussian Processes (right panels). Panels obtained from 20 simulations. Bold lines represent the mean and the shaded region is confidence interval corresponding to the standard deviation.

Consider the setting with continuous variables where $c_k(\mathbf{x}_k) = 0.5(\mathbf{x}_k - \mathbf{x}_d)^T \mathbf{W}(\mathbf{x}_k - \mathbf{x}_d)$ and where $p_{k|k-1}^{(x)} = \mathcal{N}(\mathbf{A}\mathbf{x}_{k-1} + \mathbf{B}\mathbf{u}_k, \Sigma)$, $q_{k|k-1}^{(x)} = \mathcal{N}(\mathbf{x}_d, \mathbf{R})$, $q_{k|k-1}^{(u)} = \mathcal{N}(\mathbf{u}_d, \mathbf{Q})$, with $\mathbf{W} \in \mathbb{R}^{n \times n}$, $\Sigma \in \mathbb{R}^{n \times n}$, $\mathbf{R} \in \mathbb{R}^{n \times n}$ and $\mathbf{Q} \in \mathbb{R}^{p \times p}$ being positive definite matrices and with $\mathbf{x}_d \in \mathcal{X}$ and $\mathbf{u}_d \in \mathcal{U}$ being constant vectors. An analytical solution when $\mathbf{W} = 0$ was found in Pegueroles and Russo (2019). Following similar arguments, the optimal policy in (7) - (9) becomes

$$p_{k|k-1}^{(u)*} = \mathcal{N}(\boldsymbol{\mu}_k^*, \boldsymbol{\Sigma}_k^*) \quad (11)$$

with $\boldsymbol{\mu}_k^*$ and $\boldsymbol{\Sigma}_k^*$ given by the following backward recursion for $k = 1 : N - 1$ (starting with $\mathbf{S}_N = 0$)

$$\begin{aligned} \mathbf{S}_k &= \mathbf{A}^T (\bar{\mathbf{S}}_{k+1} - \bar{\mathbf{S}}_{k+1} \mathbf{B} (\mathbf{Q}^{-1} + \mathbf{B}^T \bar{\mathbf{S}}_{k+1} \mathbf{B})^{-1} \mathbf{B}^T \bar{\mathbf{S}}_{k+1}) \mathbf{A}, \\ \bar{\mathbf{S}}_k &= \mathbf{S}_k + \mathbf{R}^{-1} + \mathbf{W}, \\ \boldsymbol{\Sigma}_k^* &= (\mathbf{Q}^{-1} + \mathbf{B}^T \bar{\mathbf{S}}_k \mathbf{B})^{-1}, \\ \boldsymbol{\mu}_k^* &= -\boldsymbol{\Sigma}_k^* \mathbf{B}^T \bar{\mathbf{S}}_k \mathbf{A} \mathbf{x}_{k-1} + \boldsymbol{\Sigma}_k^* (\mathbf{B}^T \bar{\mathbf{S}}_k \mathbf{x}_d + \mathbf{Q}^{-1} \mathbf{u}_d). \end{aligned} \quad (12)$$

See the appendix for the derivations.

Running Example (continue). We now use Theorem 1 (and hence Algorithm 1) to swing-up the target pendulum introduced in the previous part of the example. The cost associated to this control task is given in (5). For reasons that will be clear later, for both the continuous and discrete settings described above, at each k we sampled the control input from the policy computed (given \mathbf{x}_{k-1}) via Algorithm 1 with $N = 1$. As shown in Figure 1, in both the continuous and discrete settings, the policy $p_{k|k-1}^{(u)*}$ computed via Algorithm 1 stabilized the target pendulum. In the figure, the behavior is shown for the angular position of the controlled pendulum when the control input is sampled, at each k , from $p_{k|k-1}^{(u)*}$. See our github for the implementation details at <https://tinyurl.com/46uccxsf>.

3.2 Tackling the Inverse Control Problem

First, we give a result to reconstruct, via a convex problem, $\bar{c}_k(\cdot)$ by observing a sequence of states sampled from $p_{k|k-1}^{(x)}$ when the control inputs sampled from $p_{k|k-1}^{(u)*}$ are applied. Then, we build on this result to reconstruct $c_k(\cdot)$. We let Assumption 2 hold and let $\{(\hat{\mathbf{x}}_{k-1}, \hat{\mathbf{u}}_k)\}_{1:M}$ be the observed data pairs. We consider the likelihood function of $\mathbf{w} = [\mathbf{w}_1^T, \dots, \mathbf{w}_M^T]^T$

$$L(\mathbf{w}) := \prod_{k=1}^M \frac{\bar{q}_{k|k-1}^{(u)}(\hat{\mathbf{x}}_{k-1}, \hat{\mathbf{u}}_k) \exp\left(\sum_{\mathbf{x}_k} p_k(\mathbf{x}_k | \hat{\mathbf{x}}_{k-1}, \hat{\mathbf{u}}_k) \mathbf{w}_k^T \mathbf{h}(\mathbf{x}_k)\right)}{\sum_{\mathbf{u}_k} \bar{q}_{k|k-1}^{(u)}(\hat{\mathbf{x}}_{k-1}, \mathbf{u}_k) \exp\left(\sum_{\mathbf{x}_k} p_k(\mathbf{x}_k | \hat{\mathbf{x}}_{k-1}, \mathbf{u}_k) \mathbf{w}_k^T \mathbf{h}(\mathbf{x}_k)\right)}, \quad (13)$$

where

$$\begin{aligned} \bar{q}_{k|k-1}^{(u)}(\mathbf{x}_{k-1}, \mathbf{u}_k) &:= q(\mathbf{u}_k | \mathbf{x}_{k-1}) \\ &\exp(-D_{\text{KL}}(p(\mathbf{x}_k | \mathbf{x}_{k-1}, \mathbf{u}_k) \parallel q(\mathbf{x}_k | \mathbf{x}_{k-1}, \mathbf{u}_k))). \end{aligned} \quad (14)$$

and where we used the shorthand notation $p_k(\mathbf{x}_k | \hat{\mathbf{x}}_{k-1}, \hat{\mathbf{u}}_k)$, $p_k(\mathbf{x}_k | \hat{\mathbf{x}}_{k-1}, \mathbf{u}_k)$ and $q_k(\mathbf{u}_k | \hat{\mathbf{x}}_{k-1})$ to denote $p_k^{(x)}(\mathbf{x}_k | \mathbf{x}_{k-1} = \hat{\mathbf{x}}_{k-1}, \mathbf{u}_k = \hat{\mathbf{u}}_k)$, $p_k^{(x)}(\mathbf{x}_k | \mathbf{x}_{k-1} = \hat{\mathbf{x}}_{k-1}, \mathbf{u}_k)$ and $q_k^{(u)}(\mathbf{u}_k | \mathbf{x}_{k-1} = \hat{\mathbf{x}}_{k-1})$, respectively. The next result is related to what was independently reported in Dvijotham and Todorov (2010) in a different context (see Remark 11) and gives the maximum likelihood estimate for \mathbf{w} .

Theorem 2 *Let Assumption 2 hold and let the observed data pairs be $\{(\hat{\mathbf{x}}_{k-1}, \hat{\mathbf{u}}_k)\}_{1:M}$, with $\hat{\mathbf{x}}_k \sim p_{k|k-1}^{(x)}$, $\hat{\mathbf{u}}_k \sim p_{k|k-1}^{(u)*}$ and where $p_{k|k-1}^{(u)*}$ is from Theorem 1. Then, the maximum likelihood estimate for \mathbf{w} with likelihood function (13) is obtained by solving the convex problem*

$$\begin{aligned} \mathbf{w}^* &:= [\mathbf{w}_1^{*T}, \dots, \mathbf{w}_M^{*T}]^T \in \\ \arg \min_{\mathbf{w}} &\left\{ \sum_{k=1}^M \left(-\mathbb{E}_{p(\mathbf{x}_k | \hat{\mathbf{x}}_{k-1}, \hat{\mathbf{u}}_k)} [\mathbf{w}_k^T \mathbf{h}(\mathbf{x}_k)] \right. \right. \\ &+ \ln \left(\sum_{\mathbf{u}_k} \bar{q}_{k|k-1}^{(u)}(\hat{\mathbf{x}}_{k-1}, \mathbf{u}_k) \right. \\ &\left. \left. \exp(\mathbb{E}_{p(\mathbf{x}_k | \hat{\mathbf{x}}_{k-1}, \mathbf{u}_k)} [\mathbf{w}_k^T \mathbf{h}(\mathbf{x}_k)]) \right) \right\}, \end{aligned} \quad (15)$$

where $\bar{q}_{k|k-1}^{(u)}(\cdot, \cdot)$ is defined in (14).

Before giving the proof, we make the following

Remark 10 In Theorem 2, M , the number of observed data pairs $(\hat{\mathbf{x}}_{k-1}, \hat{\mathbf{u}}_k)$, can be different from the time horizon, N , of the forward control problem (Problem 1). This is useful when, as in e.g., our running example, observed data are obtained from multiple experiments.

PROOF. Assumption 2, together with the fact that the observed actions are sampled from the policy of Algorithm 1 implies that sequence of control inputs $\{\hat{\mathbf{u}}_k\}_{1:M}$ are determined by sampling, at each k , from the pmf

$$p_{k|k-1}^{(u)\star} = \frac{\bar{q}_{k|k-1}^{(u)}(\hat{\mathbf{x}}_{k-1}, \mathbf{u}_k) \exp(\mathbb{E}_{p_k(\mathbf{x}_k|\hat{\mathbf{x}}_{k-1}, \mathbf{u}_k)}[\mathbf{w}_k^T \mathbf{h}(\mathbf{x}_k)])}{\sum_{\mathbf{u}_k} \bar{q}_{k|k-1}^{(u)}(\hat{\mathbf{x}}_{k-1}, \mathbf{u}_k) \exp(\mathbb{E}_{p_k(\mathbf{x}_k|\hat{\mathbf{x}}_{k-1}, \mathbf{u}_k)}[\mathbf{w}_k^T \mathbf{h}(\mathbf{x}_k)])}. \quad (16)$$

This leads to the likelihood function in (13). We find

$$\mathbf{w}^\star \in \arg \max_{\mathbf{w}} L(\mathbf{w})$$

by minimizing the negative log-likelihood $-\log L(\mathbf{w})$. In turn, the negative log-likelihood can be written as

$$\begin{aligned} & \sum_{k=1}^M (-\ln(\bar{q}_{k|k-1}^{(u)}(\hat{\mathbf{x}}_{k-1}, \hat{\mathbf{u}}_k))) \\ & - \sum_{\mathbf{x}_k} p_k(\mathbf{x}_k | \hat{\mathbf{x}}_{k-1}, \hat{\mathbf{u}}_k) \mathbf{w}_k^T \mathbf{h}(\mathbf{x}_k) \\ & + \sum_{k=1}^M \ln \left(\sum_{\mathbf{u}_k} \bar{q}_{k|k-1}^{(u)}(\hat{\mathbf{x}}_{k-1}, \mathbf{u}_k) \cdot \right. \\ & \left. \exp \left(\sum_{\mathbf{x}_k} p_k(\mathbf{x}_k | \hat{\mathbf{x}}_{k-1}, \mathbf{u}_k) \mathbf{w}_k^T \mathbf{h}(\mathbf{x}_k) \right) \right) \end{aligned} \quad (17)$$

In (17) the term $\bar{q}_{k|k-1}^{(u)}(\cdot, \cdot)$ is defined in (14). Hence, minimizing the negative log-likelihood results into the following unconstrained optimization problem:

$$\min_{\mathbf{w}} -\log L(\mathbf{w}), \quad (18)$$

where $-\log L(\mathbf{w})$ is given in (17). Moreover, the first term in the cost function does not depend on the decision variable \mathbf{w} . Hence, such term can be removed from the formulation of the problem and this yields (15). Problem's convexity follows from the cost function being a convex combination of a linear function and the log-sum-exponential function (which is convex). \square

Remark 11 Following Theorem 2, the estimated $\bar{c}_k(\mathbf{x}_k)$, say $\bar{c}_k^\star(\mathbf{x}_k)$, is given by $\bar{c}_k^\star(\mathbf{x}_k) = -\mathbf{w}_k^{\star T} \mathbf{h}(\mathbf{x}_k)$. As in Dvijotham and Todorov (2010) in Theorem 2 we exploit the fact that the optimal solution from Theorem 1 belongs to the exponential family. In Dvijotham

and Todorov (2010) the framework of linearly solvable MDPs is exploited, which relies on the assumption that $p_k^{(x)}(\mathbf{x}_k | \mathbf{u}_k, \mathbf{x}_{k-1}) p_k^{(u)}(\mathbf{u}_k | \mathbf{x}_{k-1}) = p(\mathbf{x}_k | \mathbf{x}_{k-1})$ and $q_k^{(x)}(\mathbf{x}_k | \mathbf{u}_k, \mathbf{x}_{k-1}) q_k^{(u)}(\mathbf{u}_k | \mathbf{x}_{k-1}) = q(\mathbf{x}_k | \mathbf{x}_{k-1})$. This assumption is not required in our result.

Remark 12 The problem in (15) is an unconstrained convex optimization problem with a twice differentiable cost. Constraints on the \mathbf{w}_k 's can be added to the problem to capture additional desired properties of the cost.

Consider the situation where in Theorem 2 at each k the policy $p_{k|k-1}^{(u)\star}$ is obtained from Theorem 1 with $N = 1$. In this case, the result provides an estimate of the cost $c_k(\cdot)$. Next, we consider the case where the cost, which we simply denote by $c(\cdot)$, is stationary.

Corollary 1 Let Assumption 2 hold, the cost be stationary and $p_{k|k-1}^{(u)\star}$ be the policy obtained at each k from Theorem 1 with $N = 1$. Then, $c^\star(\mathbf{x}_k) = -\mathbf{w}_s^{\star T} \mathbf{h}(\mathbf{x}_k)$, where \mathbf{w}_s^\star is given by:

$$\mathbf{w}_s^\star \in \arg \min_{\mathbf{w}_s} \left\{ \sum_{k=1}^M (-\mathbb{E}_{p(\mathbf{x}_k|\hat{\mathbf{x}}_{k-1}, \hat{\mathbf{u}}_k)}[\mathbf{w}_s^T \mathbf{h}(\mathbf{x}_k)]) + \sum_{k=1}^M \ln \left(\sum_{\mathbf{u}_k} \bar{q}_{k|k-1}^{(u)}(\hat{\mathbf{x}}_{k-1}, \mathbf{u}_k) \exp(\mathbb{E}_{p(\mathbf{x}_k|\hat{\mathbf{x}}_{k-1}, \mathbf{u}_k)}[\mathbf{w}_s^T \mathbf{h}(\mathbf{x}_k)]) \right) \right\}. \quad (19)$$

with $\mathbf{w}_s \in \mathbf{R}^F$ and $\bar{q}_{k|k-1}^{(u)}(\hat{\mathbf{x}}_{k-1}, \mathbf{u}_k)$ defined as in Theorem 2.

PROOF. Follows from Theorem 2 after noticing that, when $N = 1$ and the cost is stationary, Theorem 1 yields

$$p_{k|k-1}^{(u)\star} = \frac{\bar{p}_{k|k-1}^{(u)} \exp\left(-\mathbb{E}_{p_k^{(x)}(\cdot|\hat{\mathbf{x}}_{k-1}, \hat{\mathbf{u}}_k)}[c(\mathbf{X}_k)]\right)}{\sum_{\mathbf{u}_k} \bar{p}_{k|k-1}^{(u)} \exp\left(-\mathbb{E}_{p_k^{(x)}(\cdot|\hat{\mathbf{x}}_{k-1}, \hat{\mathbf{u}}_k)}[c(\mathbf{X}_k)]\right)}. \quad \square$$

Following Corollary 1, when the cost is stationary, one needs to solve an optimization problem that has as decision variable the $\mathbf{w}_s \in \mathbf{R}^F$ rather than $\mathbf{w} \in \mathbf{R}^{MF}$. Also, Corollary 1 only requires that data are collected via a greedy policy obtained at each k from Theorem 1 with $N = 1$. This is convenient as it bypasses the need to solve the backward recursion in (9).

3.2.1 Turning Corollary 1 into an Algorithm

We turn Corollary 1 into an algorithmic procedure with steps given in Algorithm 2. An algorithm for Theorem 2

can also be obtained and it is omitted here for brevity.

Algorithm 2 Pseudo-code from Corollary 1: inverse control algorithm

Inputs: observed data $\{\hat{\mathbf{u}}_k\}_{1:M}$ and $\{\hat{\mathbf{x}}_{k-1}\}_{1:M}$,
 F -dimensional features vector $\mathbf{h}(\mathbf{x}_k)$,
 $p_{k|k-1}^{(x)}$, $q_{k|k-1}^{(x)}$, $q_{k|k-1}^{(u)}$

Output: $c^*(\mathbf{x}_k)$

for $k = 1$ to M **do**
 Compute $\bar{q}_{k|k-1}^{(u)}(\hat{\mathbf{x}}_{k-1}, \mathbf{u}_k)$ using (14)

end for
 Compute \mathbf{w}_s^* by solving the problem in (19)
 $c^*(\mathbf{x}_k) \leftarrow -\mathbf{w}_s^{*T} \mathbf{h}(\mathbf{x}_k)$

3.3 Special Case

We now discuss a special case of our results, relevant for applications, when the reference pfs are uniform.

Forward problem. The KL-divergence component in the cost of Problem 1 becomes an entropic regularizer and the optimal policy in (7) then becomes

$$p_{k|k-1}^{(u)*} = \frac{\exp\left(-\mathbb{E}_{p_{k|k-1}^{(x)}}\left[\ln\left(p_{k|k-1}^{(x)}\right) + \bar{c}_k(\mathbf{X}_k)\right]\right)}{\sum_{\mathbf{u}_k} \exp\left(-\mathbb{E}_{p_{k|k-1}^{(x)}}\left[\ln\left(p_{k|k-1}^{(x)}\right) + \bar{c}_k(\mathbf{X}_k)\right]\right)}, \quad (20)$$

where $\bar{c}_k(\mathbf{x}_k) = c_k(\mathbf{x}_k) - \hat{c}_k(\mathbf{x}_k)$ and with the backward recursion in (9) becoming

$$\begin{aligned} \hat{c}_k(\mathbf{x}_k) &= \ln\left(\sum_{\mathbf{u}_k} \exp\left(-\mathbb{E}_{p_{k+1|k}^{(x)}}\left[\ln\left(p_{k+1|k}^{(x)}\right) + \bar{c}_{k+1}(\mathbf{X}_{k+1})\right]\right)\right), \\ \mathbb{E}_{p_{N+1|N}^{(x)}}\left[\ln\left(p_{N+1|N}^{(x)}\right) + \bar{c}_{N+1}(\mathbf{X}_{N+1})\right] &= 0. \end{aligned}$$

Inverse problem. Since in the optimal policy is now the one in (20), the problem in (15) becomes

$$\begin{aligned} \arg \min_{\mathbf{w}} \left\{ \sum_{k=1}^M \left(-\mathbb{E}_{p(\mathbf{x}_k | \hat{\mathbf{x}}_{k-1}, \hat{\mathbf{u}}_k)} \left[\mathbf{w}_k^T \mathbf{h}(\mathbf{x}_k) \right] \right. \right. \\ \left. \left. + \ln \left(\sum_{\mathbf{u}_k} \exp \left(\mathbb{E}_{p(\mathbf{x}_k | \hat{\mathbf{x}}_{k-1}, \mathbf{u}_k)} \left[-\ln(p(\mathbf{x}_k | \hat{\mathbf{x}}_{k-1}, \mathbf{u}_k)) \right. \right. \right. \right. \\ \left. \left. \left. + \mathbf{w}_k^T \mathbf{h}(\mathbf{x}_k) \right] \right) \right) \right\}. \end{aligned}$$

Table 1

Time taken by Algorithm 2 to reconstruct the cost and comparison with Max-Ent (VI) and IHMCE (Soft-VI and MCS). The table also reports the discrepancy between the original and the reconstructed costs. Results obtained from 10 experiments. Bold: the best values for each column.

Method	Best Case	Worst Case	Average	Discrepancy
Algorithm 2	32.2 sec	1.05 min	40 sec	0.00162
Max-Ent with VI (Zhou et al., 2018)	15 mins	40 mins	28 mins	0.124
IHMCE with soft VI and MCS (Ziebart et al., 2008)	10 mins	36 mins	25 mins	0.00467

Running Example (continue). In this final part of the example we show the application of Algorithm 2 when this is leveraged to reconstruct the cost in (5) that was given as an input to Algorithm 1. Continuous and discrete settings are discussed separately. For the discrete setting we give a comparison with Ziebart et al. (2008); Zhou et al. (2018). See <https://tinyurl.com/46uccxsf> for details.

Discrete setting. We used approximately 300 data pairs collected from a single simulation of the target pendulum controlled via the policy computed in the previous part of the running example (from this dataset, we removed the points where there were discontinuities due to angle wrapping). These were the observed data given as an input to Algorithm 2. Also, we defined the features as $\mathbf{h}(\mathbf{x}_k) = [|\theta_k - \theta_d|, |\omega_k - \omega_d|]^T$ and obtained from Algorithm 2 (using CVX Diamond and Boyd (2016) to solve the optimization problem) the weights $\mathbf{w}_s^* = [-6.09, -4.48]^T$. Hence, in accordance with Corollary 1, we obtained $c^*(\mathbf{x}_k) = 6.09|\theta_k - \theta_d| + 4.48|\omega_k - \omega_d|$. Then, we used this cost as input for Algorithm 1 (again with $N = 1$) to solve the forward control problem. As shown in Figure 2 (left panel) the policy computed using $c^*(\cdot)$ effectively stabilizes the pendulum. To further validate our results, we used Algorithm 2 with the same dataset described above but with $\mathbf{h}(\mathbf{x}_k) = [1 - \exp(-(\cos(\theta_k) - 1)^2), 1 - \exp(-\omega_k^2)]$. This time we performed 10 experiments. For each experiment, the algorithm provided a set of weights and the time taken by Algorithm 2 to output the weights is summarized in Table 1 (first line). We also quantified the similarity between the original cost and the reconstructed cost. To this aim, we normalized both the original cost and the cost reconstructed via Algorithm 2 and then used the KL divergence to quantify their discrepancy. This measure of discrepancy, which is averaged across the 10 experiments, is also shown in Table 1 (last column). In Figure 3 (top-left) the reconstructed cost is shown for a set of randomly selected weights across the experiments ($\mathbf{w}_s^* = [-1913.3, -3.2]^T$). Finally, given this set of weights we used the corresponding reconstructed cost as input for Algorithm 1 and the results are shown in Figure 2 (middle panel).

Benchmarking Algorithm 2. By using the setting introduced so far, we now present a comparison between the results obtained via Algorithm 2 with the Maximum Entropy-IRL algorithm (MaxEnt for short in what follows) from Ziebart et al. (2008) and the Infinite Time Horizon Maximum Causal Entropy IRL (IHMCE) from Zhou et al. (2018). Both these methods rely on discretized action/state spaces and assume (as also required by Algorithm 2) a linear parametrization in a set of features. Additionally, these methods also assume that the policy for which the cost is reconstructed is a soft-max (see Remark 7 for a discussion on this point and at the end of Section 1.1). The results for MaxEnt and IHMCE were obtained by using the last set of features introduced above and the same data that were used as input to Algorithm 2. Fully documented code implementing MaxEnt and IHMCE is also available at <https://tinyurl.com/46uccxsf>, together with a test case validating our implementation on the grid-world from (Sutton and Barto, 1998, Chapter 3). With our first set of experiments we aimed at reconstructing the pendulum cost using MaxEnt, which foresees both forward and backward pass (FP and BP) steps. Our experiments revealed that, for the pendulum of this running example, $3.75e^{10}$ iterations were required for a single BP step to converge and this made the approach infeasible for the application. The high computation cost of the BP step was already noted in Zhou et al. (2018) where it was also proposed to use Value Iteration (VI) rather than BP to improve the computational aspect. Hence, inspired by this, we then implemented a version of MaxEnt with VI. The average discrepancy between the cost reconstructed with this algorithm and the original cost across 10 experiments is shown in Table 3, together with the corresponding computation time (one representative cost, obtained by randomly selecting one of the weight vectors from the 10 experiments is shown in the bottom-left panel of Figure 3). Based on these findings, we then implemented the IHMCE algorithm from Zhou et al. (2018) that makes use of soft VI and Monte Carlo Simulations (MCS). Again, we computed the average discrepancy across 10 experiments and recorded the computation times. The results are also given in Table 3 and a representative cost is shown in Figure 3 (bottom-right). In summary, our numerical studies illustrate that Algorithm 2 is both significantly faster than Max-Ent (with VI) and IHMCE (with soft VI and MCS) and, at the same time, achieves lower cost discrepancy.

Continuous setting. Again, we used a dataset of 300 data-points collected from a single simulation where the target pendulum was controlled by the policy from Algorithm 1 as described in the previous part of the example. This time we used as features vector $\mathbf{h}(\mathbf{x}_k) = [(\cos(\theta_k) - \cos(0))^2, (\cos(\theta_k) - \cos(\pi))^2]^T$. When this vector was given as an input to Algorithm 2 (using again CVX to solve the problem) the weights we obtained were $\mathbf{w}_s^* = [-13.66, 8.50]^T$ so that $c^*(\mathbf{x}_k) =$

$13.66(\cos(\theta_k) - \cos(0))^2 - 8.50(\cos(\theta_k) - \cos(\pi))^2$. Note that the first term in $c^*(\cdot)$ conveniently drives the pendulum towards the unstable equilibrium while the second term is pushing it away from the stable equilibrium in π , consistently with the cost in (5). Again, we then gave $c^*(\cdot)$ as an input to Algorithm 1 and verified that it was in fact able to swing-up the pendulum. The numerical results are reported in Figure 2 (right panel).

4 Application Example

We use our results to tackle an application involving routing unicycle robots in an environment with obstacles. Specifically, we consider two scenarios: in Scenario 1, the robot moves in an environment without obstacles and needs to achieve a desired destination; (ii) in Scenario 2, the robot needs to reach the destination while avoiding obstacles. For both scenarios, we first use Algorithm 1 to compute a policy routing the robot. Then, we leverage Algorithm 2 to reconstruct the navigation cost from observed robot trajectories. The results are validated both via simulations and via real hardware experiments, leveraging the *Robotarium* platform that offers both a hardware infrastructure and a high-fidelity simulator Wilson et al. (2020). The robots in the Robotarium are unicycles of dimensions $11\text{cm} \times 8.5\text{cm} \times 7.5\text{cm}$ (width, length, height) and these can move within a rectangular *work area* of $3\text{m} \times 2\text{m}$. The platform is equipped with cameras with a top view to track the robots' positions. Further, the Robotarium allows users to consider for control design a single integrator dynamics rather than the unicycle dynamics (the platform provides support functions to map single integrator dynamics to the unicycle dynamics). Hence, the dynamics of the robot we want to control is $\mathbf{x}_k = \mathbf{x}_{k-1} + \mathbf{u}_k dt$, where $\mathbf{x}_k = [p_{x,k}, p_{y,k}]^T$ is the position of the robot at time-step k , $\mathbf{u}_k = [v_{x,k}, v_{y,k}]^T$ is the input vector of velocities (in the platform, each of the components are constrained to have modulus less than 0.5m/s) and $dt = 0.033\text{s}$ is the Robotarium time-step.

For the application of our results we set $\mathbf{x}_k \in \mathcal{X} := [-1.5, 1.5] \times [-1, 1]$ and $\mathbf{u}_k \in \mathcal{U} := [-0.5, 0.5] \times [-0.5, 0.5]$. Moreover, in our experiments we emulated measurement noise for the robot position that we assumed to be Gaussian as in e.g., Yoo et al. (2016). Thus, $p_{k|k-1}^{(x)}$ is given by $\mathcal{N}(\mathbf{x}_{k-1} + \mathbf{u}_k dt, \Sigma)$, where we set

$$\Sigma = \begin{bmatrix} 0.001 & 0.0002 \\ 0.0002 & 0.001 \end{bmatrix}.$$

Given this set-up, we discuss separately the scenarios.

Scenario 1. The desired destination for the robot, where it needs to stop, is $\mathbf{x}_d = [-1.4, -0.9]^T$, in the bottom-left corner of the Robotarium work area. Consequently, for the FOC we set $c(\mathbf{x}_k) = 0.5(\mathbf{x}_k - \mathbf{x}_d)^T(\mathbf{x}_k - \mathbf{x}_d)$, $q_{k|k-1}^{(x)} = \mathcal{N}(\mathbf{x}_d, \Sigma_x)$ and $q_{k|k-1}^{(u)} = \mathcal{N}(\mathbf{u}_d, \Sigma_u)$, where

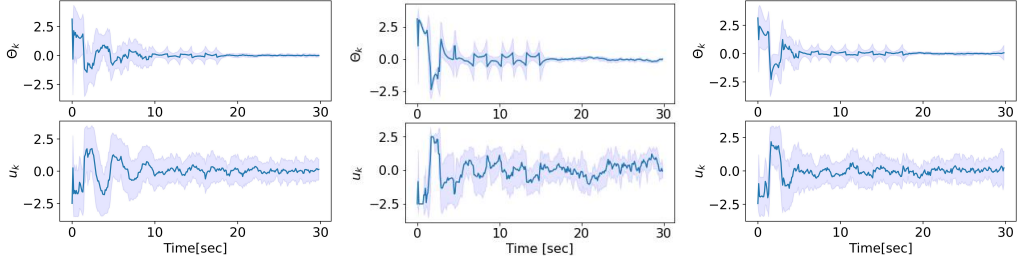


Fig. 2. Angular position and control input of the target Pendulum when the pf is estimated via the histogram filter (left and middle panels) and Gaussian Processes (right panels). Figures obtained from 20 simulations, using $c^*(\cdot)$ as an input to Algorithm 1. Bold lines represents the mean; the shaded region is confidence interval corresponding to the standard deviation.

$\mathbf{u}_d = [0, 0]^T$, $\Sigma_x = 0.003 \cdot \mathbf{I}_2$ and $\Sigma_u = 0.007 \cdot \mathbf{I}_2$ (\mathbf{I}_2 is the 2×2 identity matrix). We then used the policy in (11) - (12) to control the robot and the results are in Figure 4 (top-left panel). In the figure, the behavior of the robot controlled with our policy is shown when this starts from 4 different positions. Next, we used the data pairs collected from the 4 experiments to reconstruct the cost. We used Algorithm 2 with a 15-dimensional feature vector ($F = 15$) and the h_i 's given by $h_i(\mathbf{x}_k) = (\mathbf{x}_k - \mathbf{o}_i)^T (\mathbf{x}_k - \mathbf{o}_i)$, where the \mathbf{o}_i 's were the coordinates of the points in the work area shown in Figure 4 (top-right). The figure also shows the weights returned by Algorithm 2 for each of the features. The weights were obtained by adding a non-positivity constraint on \mathbf{w}_s in the formulation of (19), leveraging the fact that the optimization problem (which we solved via CVX) would still be convex (see Remark 12). The reconstructed cost is also shown in the bottom-left panel of Figure 4. We then gave back this cost to Algorithm 1 to verify if the robot would still be able to achieve the destination. We performed these experiments by letting the robot start in positions that were different from the ones contained in the dataset used to estimate the cost. The results in Figure 4 (bottom-right) confirm successful routing of the robot. See our github for the documented

code associated to the experiments described above.

Scenario 2. We decided not to build a target pf and set $q_{k|k-1}^{(x)}$ and $q_{k|k-1}^{(u)}$ to be uniform. Further, we discretized \mathcal{U} in a 5×5 grid. For the forward control problem, we used $c(\mathbf{x}_k) = 30(\mathbf{x}_k - \mathbf{x}_d)^2 + 20 \sum_{i=1}^n g_i(\mathbf{x}_k) + 10b(\mathbf{x}_k)$, where: (i) \mathbf{x}_d is the desired goal/destination for the robot so that the first term in the cost promotes reaching the goal; (ii) n is the number of obstacles; (iii) the terms in the sum promote obstacle avoidance; (iv) the last term is a cost associated to the boundaries of the Robotarium work area (the specific expression of this component of the cost is given on our github). We picked the g_i 's as

$$g_i(\mathbf{x}_k) := \frac{\exp(-0.5(\mathbf{x}_k - \mathbf{o}_i)^T \Sigma_o^{-1} (\mathbf{x}_k - \mathbf{o}_i))}{\sqrt{(2\pi)^2 \det(\Sigma_o)}}, \quad (21)$$

with \mathbf{o}_i being the coordinates of the barycenter of the i -th obstacle and Σ_o being the co-variance matrix. See our github for the specific values of these parameters. A plot of the cost function is given in Figure 5 (top-left panel). We then used Algorithm 1 with $N = 1$ to control the robot. In our implementation of the algorithm, available at our github, the integrals to compute the expectations in (20) were estimated via Monte Carlo sampling and, since $p_{k|k-1}^{(x)}$ is Gaussian, we used the analytic expression for the entropy. We ran 4 experiments from different initial robot positions (the same used in Scenario 1) and, for each of the experiments we recorded the robot trajectories. In all the experiments, as shown in the top-right panel of Figure 5, the algorithm properly routed the robot to the destination while avoiding the obstacles. A video recording from an experiment is also given on our github. Next, we leveraged Algorithm 2 to reconstruct the cost using the data pairs collected from the 4 experiments above. We used a 16-dimensional features vector (i.e., $F = 16$), with the first h_i equal to $(\mathbf{x}_k - \mathbf{x}_d)^2$ and with the other h_i 's being Gaussians of the form (21) but centered around the 15 uniformly distributed points in the work area of Figure 4 (top-right). Again, we used CVX to solve the underlying optimization problem and, conveniently, this returned a vector of weights that would assign high values in magnitude to weights that corresponded to the obstacles and to the final destina-

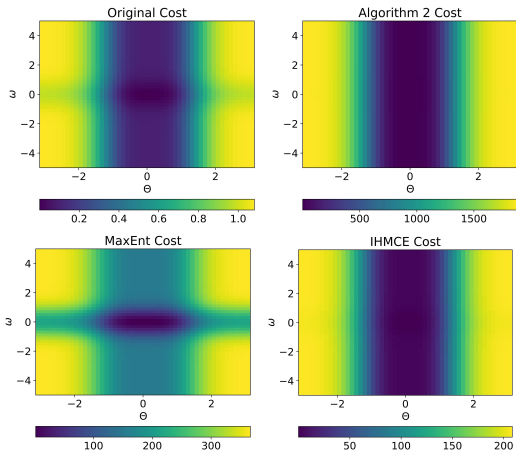


Fig. 3. Top left: original cost function. In the other panels the cost reconstructed via: Algorithm 2 (top-right), MaxEnt (bottom-left) and IHMCE (bottom-right).

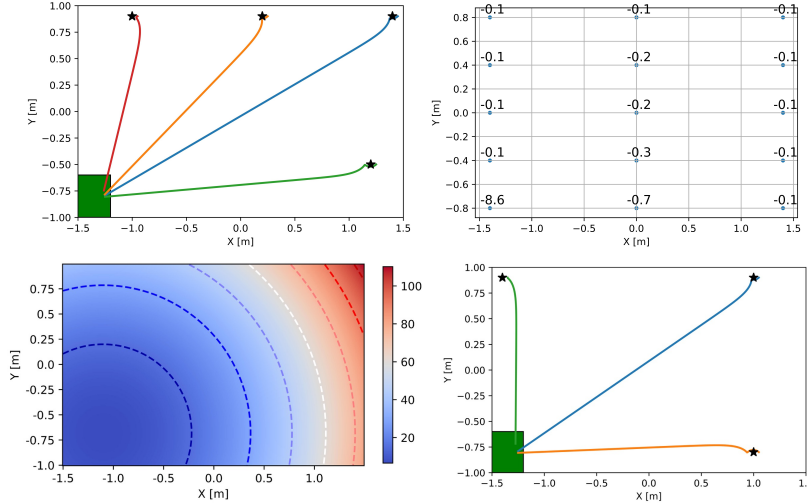


Fig. 4. Top-left: robot trajectories starting from different initial positions (\star) when the policy in (11) - (12) is used (with $N = 1$). Top-right: the \mathbf{o}_i 's together with the weights obtained via Algorithm 2. Bottom: reconstructed cost (left) and robot trajectories when Algorithm 1 is used with this cost. Robot starts from initial positions that are different from those in the top panel.

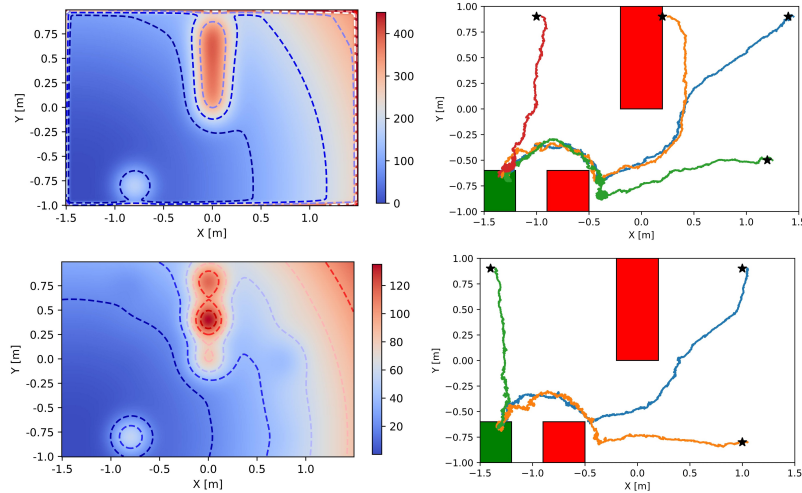


Fig. 5. Top-left: cost for the FOC problem. Top-right: robot trajectories when the policy from Algorithm 1 is used (same initial positions and destination of Scenario 1). Bottom panels: cost reconstructed via Algorithm 2 (left) and robot trajectories when Algorithm 1 is used with the estimated cost. Robots start from initial positions that are different from these in the top panel.

tion. See the github for the values. Finally, we again gave back the reconstructed cost as an input to Algorithm 1 with the aim of verifying if the robot would still be able to achieve the destination, this time also avoiding obstacles. As for Scenario 1, we performed these experiments by letting the robots start from new initial positions and the results in Figure 5 confirm successful routing and obstacle avoidance. See <https://tinyurl.com/46uccxsf> for a recording from one experiment.

5 Conclusions

We considered the problem of reconstructing the possibly non-convex and non-stationary cost driving the ac-

tions of an agent from observations of its interactions with a nonlinear, non-stationary, and stochastic environment. By leveraging probabilistic descriptions that can be derived both directly from the data and from first-principles, we presented a result to tackle the inverse problem by solving a convex optimization problem. To obtain this result we also studied a forward control problem with randomized policies as decision variables. The results were also turned into algorithmic procedures with the code for our experiments made openly available. The effectiveness of our algorithms was experimentally evaluated via in-silico and hardware validations. As part of our future work, we aim to: (i) combine the reproducing kernel Hilbert space and multiple kernel learning frameworks with our approach; (ii) use alterna-

tive cost parametrizations that can be tackled via e.g., distributed solution methods Notarnicola et al. (2021); (iii) study constrained versions of Problem 1. We also seek to: (i) engineer a principled feedback loop where the outcome of the inverse problem promotes exploration in the forward problem Karasev et al. (2012); (ii) following our discussion in Section 2.2, formalize, and exploit, links between our problem formulations, fully probabilistic design and optimal transport Terpin et al. (2023); (iii) extend our results to multi-agent systems performing repetitive tasks Nair et al. (2022); Bertsekas (2021) and to online settings Guan et al. (2014). From the applications viewpoint, we aim to design incentive schemes in sharing economy settings Crisostomi et al. (2020).

Acknowledgments

EG and GR would like to thank Dr. Guy and Prof. Kárný (Institute of Information Theory and Automation at the Czech Academy of Sciences) for the insightful discussions on a preliminary version of the results presented here. GR also wishes to thank Prof. Chiuso (Univ. of Padova) for the interesting insights on guided exploration. The authors also wish to thank the AE and two anonymous reviewers who made several helpful comments and suggestions. These inputs led to improvements over the originally submitted manuscript.

A Appendix

A.1 Proof of Theorem 1

Step 1. By means of Lemma 1, Problem 1 can be recast as the sum of the following two sub-problems:

$$\begin{aligned} \min_{\{p_{k|k-1}^{(u)}\}_{1:N-1}} & \left\{ D_{\text{KL}}(p_{0:N-1} \parallel q_{0:N-1}) \right. \\ & \left. + \sum_{k=1}^{N-1} \mathbb{E}_{\bar{p}_{k-1:k}} \left[\mathbb{E}_{p_{k|k-1}^{(x)}} [c_k(\mathbf{X}_k)] \right] \right\} \\ \text{s.t. } & p_{k|k-1}^{(u)} \in \mathcal{D} \quad \forall k \in 1:N-1, \end{aligned} \quad (\text{A.1a})$$

and

$$\begin{aligned} \min_{p_{N|N-1}^{(u)}} & \left\{ \mathbb{E}_{\bar{p}_{N-1}} [D_{\text{KL}}(p_{N|N-1} \parallel q_{N|N-1}) \right. \\ & \left. + \mathbb{E}_{p_{N|N-1}} [c_N(\mathbf{X}_N)] \right\} \\ \text{s.t. } & p_{N|N-1}^{(u)} \in \mathcal{D}. \end{aligned} \quad (\text{A.1b})$$

Hence, to solve Problem 1 we solve (A.1b) and take its solution into account in (A.1a). We let $\mathcal{C}_N \{p_{N|N-1}^{(u)}\} :=$

$D_{\text{KL}}(p_{N|N-1} \parallel q_{N|N-1}) + \mathbb{E}_{p_{N|N-1}} [c_N(\mathbf{X}_N)]$. Then, the minimum of (A.1b) is $\mathbb{E}_{\bar{p}_{N-1}} [\mathcal{C}_N \{p_{N|N-1}^{(u)*}\}]$, with

$$\begin{aligned} p_{N|N-1}^{(u)*} & \in \arg \min_{p_{N|N-1}^{(u)}} \left\{ D_{\text{KL}}(p_{N|N-1} \parallel q_{N|N-1}) \right. \\ & \left. + \mathbb{E}_{p_{N|N-1}} [\bar{c}_N(\mathbf{X}_N)] \right\} \\ \text{s.t. } & p_{N|N-1}^{(u)} \in \mathcal{D}, \end{aligned} \quad (\text{A.2})$$

where we set $\bar{c}_N(\mathbf{x}_N) := c_N(\mathbf{x}_N) + \hat{c}_N(\mathbf{x}_N)$, $\hat{c}_N(\mathbf{x}_N) = 0$. This corresponds to the recursion in (9) at $k = N$.

Step 2. The constraint in (A.2) is linear in the decision variable and we show convexity of the problem by showing that its cost functional is convex. Note that:

$$\begin{aligned} \mathcal{C}_N \{p_{N|N-1}^{(u)}\} & = \\ & D_{\text{KL}}(p_{N|N-1} \parallel q_{N|N-1}) + \mathbb{E}_{p_{N|N-1}} [\bar{c}_N(\mathbf{X}_N)] \\ & = \mathbb{E}_{p_{N|N-1}^{(u)}} \left[D_{\text{KL}}(p_{N|N-1}^{(x)} \parallel q_{N|N-1}^{(x)}) \right. \\ & \left. + \mathbb{E}_{p_{N|N-1}^{(x)}} [\bar{c}_N(\mathbf{X}_N)] \right] + D_{\text{KL}}(p_{N|N-1}^{(u)} \parallel q_{N|N-1}^{(u)}). \end{aligned}$$

Hence, the problem in (A.2) becomes

$$\begin{aligned} \min_{p_{N|N-1}^{(u)}} & \left\{ \mathbb{E}_{p_{N|N-1}^{(u)}} \left[D_{\text{KL}}(p_{N|N-1}^{(x)} \parallel q_{N|N-1}^{(x)}) \right. \right. \\ & \left. \left. + \mathbb{E}_{p_{N|N-1}^{(x)}} [\bar{c}_N(\mathbf{X}_N)] \right] \right. \\ & \left. + D_{\text{KL}}(p_{N|N-1}^{(u)} \parallel q_{N|N-1}^{(u)}) \right\} \\ \text{s.t. } & p_{N|N-1}^{(u)} \in \mathcal{D}, \end{aligned} \quad (\text{A.3})$$

which has a strictly convex cost.

Step 3. The Lagrangian of the problem in (A.3) is $\mathcal{L}(p_{N|N-1}^{(u)}, \lambda_N) = \mathbb{E}_{p_{N|N-1}^{(u)}} [D_{\text{KL}}(p_{N|N-1}^{(x)} \parallel q_{N|N-1}^{(x)}) + \mathbb{E}_{p_{N|N-1}^{(x)}} [\bar{c}_N(\mathbf{X}_N)]] + D_{\text{KL}}(p_{N|N-1}^{(u)} \parallel q_{N|N-1}^{(u)}) + \lambda_N (\sum_{\mathbf{u}_k} p_{N|N-1}^{(u)} - 1)$, where λ_N is the Lagrange multiplier corresponding to the constraint $p_{N|N-1}^{(u)} \in \mathcal{D}$. We find the optimal solution by imposing the first order stationarity conditions on $\mathcal{L}(p_{N|N-1}^{(u)}, \lambda_N)$. We start with imposing the stationarity condition with respect to $p_{N|N-1}^{(u)}$. This yields $D_{\text{KL}}(p_{N|N-1}^{(x)} \parallel q_{N|N-1}^{(x)}) + \mathbb{E}_{p_{N|N-1}^{(x)}} [\bar{c}_N(\mathbf{X}_N)] + \ln \frac{p_{N|N-1}^{(u)}}{q_{N|N-1}^{(u)}} + 1 + \lambda_N = 0$. Hence, any

candidate solution is of the form:

$$\tilde{p}_{N|N-1}^{(u)} = \frac{\bar{p}_{N|N-1}^{(u)} \exp\left(-\mathbb{E}_{p_{N|N-1}^{(x)}}[\bar{c}_N(\mathbf{X}_N)]\right)}{\exp(1 + \lambda_N)}, \quad (\text{A.4})$$

where $\bar{p}_{N|N-1}^{(u)}$ is defined as in (8). Now, by imposing the stationarity condition for $\mathcal{L}(p_{N|N-1}^{(u)}, \lambda_N)$ with respect to λ_N , we get $\sum_{\mathbf{u}_N} \bar{p}_{N|N-1}^{(u)} - 1 = 0$. Hence, we get:

$$\sum_{\mathbf{u}_N} \bar{p}_{N|N-1}^{(u)} \exp\left(-\mathbb{E}_{p_{N|N-1}^{(x)}}[\bar{c}_N(\mathbf{X}_N)]\right) = \exp(1 + \lambda_N). \quad (\text{A.5})$$

Since the problem in (A.3) is convex with a strictly convex cost functional, (A.4) and (A.5) imply Ben-Tal et al. (1988) that the unique optimal solution is

$$p_{N|N-1}^{(u)*} = \frac{\bar{p}_{N|N-1}^{(u)} \exp\left(-\mathbb{E}_{p_{N|N-1}^{(x)}}[\bar{c}_N(\mathbf{X}_N)]\right)}{\sum_{\mathbf{u}_N} \bar{p}_{N|N-1}^{(u)} \exp\left(-\mathbb{E}_{p_{N|N-1}^{(x)}}[\bar{c}_N(\mathbf{X}_N)]\right)}. \quad (\text{A.6})$$

This is the optimal solution given in (7) for $k = N$, with $\bar{c}_N(\mathbf{x}_N)$ generated via the backward recursion in (9). Moreover, the minimum of the problem in (A.3) is:

$$\begin{aligned} \mathcal{C}_N \left\{ p_{N|N-1}^{(u)*} \right\} = & \\ & - \ln \left(\sum_{\mathbf{u}_N} q_{N|N-1}^{(u)} \exp\left(-D_{\text{KL}}\left(p_{N|N-1}^{(x)} \parallel q_{N|N-1}^{(x)}\right) \right. \right. \\ & \left. \left. - \mathbb{E}_{p_{N|N-1}^{(x)}}[\bar{c}_N(\mathbf{X}_N)]\right) \right). \end{aligned}$$

Hence, the minimum for the sub-problem in (A.1b) is

$$\mathbb{E}_{\bar{p}_{N-1}} \left[\mathcal{C}_N \left\{ p_{N|N-1}^{(u)*} \right\} \right] = -\mathbb{E}_{\bar{p}_{N-1}} [\hat{c}_{N-1}(\mathbf{X}_{N-1})], \quad (\text{A.7})$$

where

$$\begin{aligned} \hat{c}_{N-1}(\mathbf{x}_{N-1}) := & \\ & \ln \left(\mathbb{E}_{q_{N|N-1}^{(u)}} \left[\exp\left(-D_{\text{KL}}\left(p_{N|N-1}^{(x)} \parallel q_{N|N-1}^{(x)}\right) \right. \right. \right. \\ & \left. \left. - \mathbb{E}_{p_{N|N-1}^{(x)}}[\bar{c}_N(\mathbf{X}_N)]\right) \right] \right). \end{aligned}$$

This is the optimal cost for $k = N$ given in part (ii) of the statement. Next, we make use of the minimum found for the sub-problem (A.1b) to solve the sub-problem corresponding to $k \in 1 : N - 1$.

Step 4. Since the problem in (2) has been split as the sum of the sub-problems in (A.1a) - (A.1b) and since the solution of (A.1b) gives the minimum (A.7), we have that Problem 1 is equivalent to

$$\begin{aligned} \min_{\{p_{k|k-1}^{(u)}\}_{1:N-1}} & \left\{ D_{\text{KL}}(p_{0:N-1} \parallel q_{0:N-1}) \right. \\ & + \sum_{k=1}^{N-1} \mathbb{E}_{\bar{p}_{k-1:k}} \left[\mathbb{E}_{p_{k|k-1}^{(x)}} [c_k(\mathbf{X}_k)] \right] \\ & \left. - \mathbb{E}_{\bar{p}_{N-1}} [\hat{c}_{N-1}(\mathbf{X}_{N-1})] \right\} \quad (\text{A.8}) \\ \text{s.t. } & p_{k|k-1}^{(u)} \in \mathcal{D} \quad \forall k \in 1 : N - 1. \end{aligned}$$

In turn, the cost of the above problem can be written as:

$$\begin{aligned} D_{\text{KL}}(p_{0:N-2} \parallel q_{0:N-2}) & + \sum_{k=1}^{N-2} \mathbb{E}_{\bar{p}_{k-1:k}} \left[\mathbb{E}_{p_{k|k-1}^{(x)}} [c_k(\mathbf{X}_k)] \right] \\ & + \mathbb{E}_{p_{0:N-2}} [D_{\text{KL}}(p_{N-1|N-2} \parallel q_{N-1|N-2})] \\ & + \mathbb{E}_{\bar{p}_{N-2:N-1}} \left[\mathbb{E}_{p_{N-1|N-2}^{(x)}} [c_{N-1}(\mathbf{X}_{N-1})] \right] \\ & - \mathbb{E}_{\bar{p}_{N-1}} [\hat{c}_{N-1}(\mathbf{X}_{N-1})], \quad (\text{A.9}) \end{aligned}$$

where we recall from Section 2.1 that $p_{N-1|N-2}^{(x)}$ is the shorthand notation for $p_{N-1}^{(x)}(\mathbf{x}_{N-1} \mid \mathbf{x}_{N-2}, \mathbf{u}_{N-1})$. Also, following e.g., (Gagliardi and Russo, 2022), for the last three terms in (A.9) we note that: (i) $D_{\text{KL}}(p_{N-1|N-2} \parallel q_{N-1|N-2})$ only depends on \mathbf{X}_{N-2} and hence $\mathbb{E}_{p_{0:N-2}} [D_{\text{KL}}(p_{N-1|N-2} \parallel q_{N-1|N-2})] = \mathbb{E}_{\bar{p}_{N-2}} [D_{\text{KL}}(p_{N-1|N-2} \parallel q_{N-1|N-2})]$; (ii) the expectation on the third line of (A.9) can be written as $\mathbb{E}_{\bar{p}_{N-2}} [\mathbb{E}_{p_{N-1|N-2}} [c_{N-1}(\mathbf{X}_{N-1})]]$, where $p_{N-1|N-2}$ is defined (in Section 2.1) as $p(\mathbf{x}_{N-1}, \mathbf{u}_{N-1} \mid \mathbf{x}_{N-2})$; (iii) the expectation in the last line of (A.9) can be recast as $\mathbb{E}_{\bar{p}_{N-2}} [\mathbb{E}_{p_{N-1|N-2}} [\hat{c}_{N-1}(\mathbf{X}_{N-1})]]$. Therefore, the last three terms in (A.9) can be written as

$$\begin{aligned} & \mathbb{E}_{\bar{p}_{N-2}} [D_{\text{KL}}(p_{N-1|N-2} \parallel q_{N-1|N-2})] \\ & + \mathbb{E}_{p_{N-1|N-2}} [\bar{c}_{N-1}(\mathbf{X}_{N-1})], \end{aligned}$$

where $\bar{c}_{N-1}(\mathbf{x}_{N-1}) := c_{N-1}(\mathbf{x}_{N-1}) - \hat{c}_{N-1}(\mathbf{x}_{N-1})$. This corresponds to the recursion (9) at time $k = N - 1$. Now, the problem in (A.8) can be again split, this time as the

sum of the following two sub-problems:

$$\begin{aligned} \min_{\{p_{k|k-1}^{(u)}\}_{1:N-2}} & \left\{ D_{\text{KL}}(p_{0:N-2} \parallel q_{0:N-2}) \right. \\ & \left. + \sum_{k=1}^{N-2} \mathbb{E}_{\bar{p}_{k-1:k}} \left[\mathbb{E}_{p_{k|k-1}^{(x)}} [c_k(\mathbf{X}_k)] \right] \right\} \\ \text{s.t. } & p_{k|k-1}^{(u)} \in \mathcal{D} \quad \forall k \in 1:N-2, \end{aligned} \quad (\text{A.10a})$$

and

$$\begin{aligned} \min_{p_{N-1|N-2}^{(u)}} & \left\{ \mathbb{E}_{\bar{p}_{N-2}} [D_{\text{KL}}(p_{N-1|N-2} \parallel q_{N-1|N-2}) \right. \\ & \left. + \mathbb{E}_{p_{N-1|N-2}} [\bar{c}_{N-1}(\mathbf{X}_{N-1})] \right\} \\ \text{s.t. } & p_{N-1|N-2}^{(u)} \in \mathcal{D}. \end{aligned} \quad (\text{A.10b})$$

Again, the sub-problem in (A.10b) is independent on the sub-problem in (A.10a) and its decision variable, i.e. $p_{N-1|N-2}^{(u)}$, is independent on \bar{p}_{N-2} . Hence the minimum is $\mathbb{E}_{\bar{p}_{N-2}} [\mathcal{C}_{N-1} \{p_{N-1|N-2}^{(u)*}\}]$, with

$$\begin{aligned} \mathcal{C}_{N-1} \{p_{N-1|N-2}^{(u)*}\} & := D_{\text{KL}}(p_{N-1|N-2} \parallel q_{N-1|N-2}) \\ & + \mathbb{E}_{p_{N-1|N-2}} [\bar{c}_{N-1}(\mathbf{X}_{N-1})], \end{aligned}$$

and $p_{N-1|N-2}^{(u)*}$ being the solution of

$$\begin{aligned} \min_{p_{N-1|N-2}^{(u)}} & \left\{ D_{\text{KL}}(p_{N-1|N-2} \parallel q_{N-1|N-2}) \right. \\ & \left. + \mathbb{E}_{p_{N-1|N-2}} [\bar{c}_{N-1}(\mathbf{X}_{N-1})] \right\} \\ \text{s.t. } & p_{N-1|N-2}^{(u)} \in \mathcal{D}. \end{aligned} \quad (\text{A.11})$$

This has the same structure as (A.2) and hence the unique optimal solution for the sub-problem in (A.11) is

$$\begin{aligned} p_{N-1|N-2}^{(u)*} & = \\ & \frac{\bar{p}_{N-1|N-2}^{(u)} \exp\left(-\mathbb{E}_{p_{N-1|N-2}^{(x)}} [\bar{c}_{N-1}(\mathbf{X}_{N-1})]\right)}{\sum_{\mathbf{u}_{N-1}} \bar{p}_{N-1|N-2}^{(u)} \exp\left(-\mathbb{E}_{p_{N-1|N-2}^{(x)}} [\bar{c}_{N-1}(\mathbf{X}_{N-1})]\right)}. \end{aligned} \quad (\text{A.12})$$

That is, (A.12) is the optimal solution given in (7) for $k = N-1$, with $\bar{c}_{N-1}(\mathbf{x}_{N-1})$ obtained via the backward recursion in (9). Moreover, the corresponding cost for the

problem in (A.10b) is $\mathbb{E}_{\bar{p}_{N-2}} [\mathcal{C}_{N-1} \{p_{N-1|N-2}^{(u)*}\}] = -\mathbb{E}_{\bar{p}_{N-2}} [\hat{c}_{N-2}(\mathbf{X}_{N-2})]$, where

$$\begin{aligned} \hat{c}_{N-2}(\mathbf{x}_{N-2}) & = \\ & \ln \left(\mathbb{E}_{q_{N-1|N-2}^{(u)}} \left[\exp \left(-D_{\text{KL}}(p_{N-1|N-2}^{(x)} \parallel q_{N-1|N-2}^{(x)}) \right) \right. \right. \\ & \left. \left. - \mathbb{E}_{p_{N-1|N-2}^{(x)}} [\bar{c}_{N-1}(\mathbf{X}_{N-1})] \right) \right]. \end{aligned}$$

This is the optimal cost for $k = N-1$ given in part (ii) of the statement. We can now draw the desired conclusions.

Step 5. By iterating Step 4, at each of the remaining time-steps in the window $1:N-2$, Problem 1 can always be split in sub-problems, where the sub-problem corresponding to the last time instant is given by:

$$\begin{aligned} \min_{p_{k|k-1}^{(u)}} & \mathbb{E}_{\bar{p}_{k-1}} [D_{\text{KL}}(p_{k|k-1} \parallel q_{k|k-1}) + \mathbb{E}_{p_{k|k-1}} [\bar{c}_k(\mathbf{X}_k)]] \\ \text{s.t. } & p_{k|k-1}^{(u)} \in \mathcal{D}, \end{aligned} \quad (\text{A.13})$$

where $\bar{c}_k(\mathbf{x}_k) := c_k(\mathbf{x}_k) - \hat{c}_k(\mathbf{x}_k)$ and,

$$\begin{aligned} \hat{c}_k(\mathbf{x}_k) & = \ln \left(\mathbb{E}_{q_{k+1|k}^{(u)}} \left[\exp \left(-D_{\text{KL}}(p_{k+1|k}^{(x)} \parallel q_{k+1|k}^{(x)}) \right) \right. \right. \\ & \left. \left. - \mathbb{E}_{p_{k+1|k}^{(x)}} [\bar{c}_{k+1}(\mathbf{X}_{k+1})] \right) \right]. \end{aligned}$$

This yields the recursion in (9) a time k . Hence, the optimal solution for the sub-problem is

$$p_{k|k-1}^{(u)*} = \frac{\bar{p}_{k|k-1}^{(u)} \exp\left(-\mathbb{E}_{p_{k|k-1}^{(x)}} [\bar{c}_k(\mathbf{X}_k)]\right)}{\sum_{\mathbf{u}_k} \bar{p}_{k|k-1}^{(u)} \exp\left(-\mathbb{E}_{p_{k|k-1}^{(x)}} [\bar{c}_k(\mathbf{X}_k)]\right)}.$$

This is the optimal solution given in (7) at time k , with $\bar{c}_k(\mathbf{x}_k)$ obtained from the backward recursion in (9). Part (i) of the result is then proved. The corresponding optimal cost at time k is $-\mathbb{E}_{\bar{p}_{k-1}} [\hat{c}_{k-1}(\mathbf{X}_{k-1})]$. Thus, the optimal cost Problem 1 is $-\sum_{k=1}^N \mathbb{E}_{\bar{p}_{k-1}} [\hat{c}_{k-1}(\mathbf{X}_{k-1})]$ and this proves part (ii) of the result. \square

A.2 Proofs of Instrumental Results

Proposition 1. Item (ii) implies that the second part of the cost in (4) is lower bounded by $-\bar{\epsilon}$ and upper bounded by 0. Hence, we need to show that (i) implies boundedness of the first component of (4). By recursively applying Lemma 1, we get that the first component of (4) can be written as $D_{\text{KL}}(p_0(\mathbf{x}_0) \parallel \tilde{q}_0(\mathbf{x}_0)) + \sum_{k=1}^N \mathbb{E}_{p_{k-1}(\mathbf{x}_{k-1})} [D_{\text{KL}}(p_{k|k-1} \parallel \tilde{q}_{k|k-1})]$. Now, (i) implies that $D_{\text{KL}}(p_0(\mathbf{x}_0) \parallel \tilde{q}_0(\mathbf{x}_0)) \leq H_0$.

Additionally, at each k , the term inside the expectation of the above expression can be written as $\mathbb{E}_{p_{k|k-1}^{(u)}} \left[D_{\text{KL}} \left(p_{k|k-1}^{(x)} \parallel \tilde{q}_{k|k-1}^{(x)} \right) \right] + D_{\text{KL}} \left(p_{k|k-1}^{(u)} \parallel \tilde{q}_{k|k-1}^{(u)} \right)$ and from (i) there exist some constant H_k such that $D_{\text{KL}} \left(p_{k|k-1}^{(x)} \parallel \tilde{q}_{k|k-1}^{(x)} \right) \leq H_k$. The desired conclusion then follows by noticing that, at each k , the term $D_{\text{KL}} \left(p_{k|k-1}^{(u)} \parallel \tilde{q}_{k|k-1}^{(u)} \right) = 0$ if $p_{k|k-1}^{(u)} = \tilde{q}_{k|k-1}^{(u)}$.

Derivations for the policy in (11) - (12). We note that, in the given setting, $D_{\text{KL}} \left(p_{k|k-1}^{(x)} \parallel q_{k|k-1}^{(x)} \right) = 0.5(\mathbf{A}\mathbf{x}_{k-1} + \mathbf{B}\mathbf{u}_k - \mathbf{x}_d)^T \mathbf{R}^{-1}(\mathbf{A}\mathbf{x}_{k-1} + \mathbf{B}\mathbf{u}_k - \mathbf{x}_d) - 0.5 \text{Tr}(\mathbf{\Sigma}(\mathbf{\Sigma}^{-1} - \mathbf{R}^{-1}))$ and $\mathbb{E}_{p_{k|k-1}^{(x)}} [c_k(\mathbf{x}_k)] = 0.5(\mathbf{A}\mathbf{x}_{k-1} + \mathbf{B}\mathbf{u}_k - \mathbf{x}_d)^T \mathbf{W}(\mathbf{A}\mathbf{x}_{k-1} + \mathbf{B}\mathbf{u}_k - \mathbf{x}_d) + 0.5 \text{Tr}(\mathbf{\Sigma}_x \mathbf{W})$. In turn, $\mathbb{E}_{p_{k|k-1}^{(x)}} [\hat{c}_k(\mathbf{X}_k)]$ can be conveniently written as:

$$\begin{aligned} \mathbb{E}_{p_{k|k-1}^{(x)}} [\hat{c}_k(\mathbf{X}_k)] &= 0.5 \text{Tr}(\mathbf{S}_k \mathbf{\Sigma}) - 0.5 \omega_k \\ &- 0.5(\mathbf{A}\mathbf{x}_{k-1} - \mathbf{B}\mathbf{u}_k)^T \mathbf{S}_k (\mathbf{A}\mathbf{x}_{k-1} (\mathbf{A}\mathbf{x}_{k-1} - \mathbf{B}\mathbf{u}_k)), \end{aligned} \quad (\text{A.14})$$

with ω_k given, for $k = 1 : N - 1$, by the following backward recursion (starting with $\omega_N = 0$)

$$\begin{aligned} \omega_k &= \ln(|\mathbf{I} + (\mathbf{B}\mathbf{Q}^{0.5})^T \bar{\mathbf{S}}_{k+1} (\mathbf{B}\mathbf{Q}^{0.5})|) + \omega_{k+1} + \text{Tr}(\mathbf{S}_{k+1} \mathbf{\Sigma}) \\ &+ \mathbf{x}_d^T (\mathbf{R}^{-1} + \mathbf{W}) \mathbf{x}_d + \mathbf{u}_d^T \mathbf{Q}^{-1} \mathbf{u}_d + \text{Tr}(\mathbf{R}^{-1} \mathbf{\Sigma}) + \text{Tr}(\mathbf{W} \mathbf{\Sigma}) \\ &+ (\mathbf{B}^T \mathbf{R}^{-1} \mathbf{x}_d + \mathbf{Q}^{-1} \mathbf{u}_d)^T \mathbf{\Sigma}_k (\mathbf{B}^T \mathbf{R}^{-1} \mathbf{x}_d + \mathbf{Q}^{-1} \mathbf{u}_d), \end{aligned}$$

and where $|\cdot|$ denotes the determinant. In the above expressions \mathbf{S}_k and $\bar{\mathbf{S}}_k$ are given, for $k = 1 : N - 1$, by the following backward recursion (starting with $\mathbf{S}_N = 0$)

$$\begin{aligned} \mathbf{S}_k &= \mathbf{A}^T (\bar{\mathbf{S}}_{k+1} - \bar{\mathbf{S}}_{k+1} \mathbf{B} \mathbf{\Sigma}_{k+1} \mathbf{B}^T \bar{\mathbf{S}}_{k+1}) \mathbf{A}, \\ \bar{\mathbf{S}}_k &= \mathbf{S}_k + \mathbf{R}^{-1} + \mathbf{W}, \\ \mathbf{\Sigma}_k^* &= (\mathbf{Q}^{-1} + \mathbf{B}^T \bar{\mathbf{S}}_k \mathbf{B})^{-1}. \end{aligned} \quad (\text{A.15})$$

The policy in (11) - (12) is then obtained by substituting in (7) and (8) the above analytical expressions for $D_{\text{KL}} \left(p_{k|k-1}^{(x)} \parallel q_{k|k-1}^{(x)} \right)$, $\mathbb{E}_{p_{k|k-1}^{(x)}} [c_k(\mathbf{x}_k)]$ and $\mathbb{E}_{p_{k|k-1}^{(x)}} [\hat{c}_k(\mathbf{X}_k)]$. Specifically, adapting the derivations of e.g., Kárný (1996), by completing the squares we get:

$$\begin{aligned} p_{k|k-1}^{(u)*} &= (2\pi |\mathbf{\Sigma}_k|)^{-0.5} \exp \left(-0.5 \left[(\mathbf{u}_k \right. \right. \\ &+ (\mathbf{\Sigma}_k (\mathbf{x}_{k-1}^T \mathbf{A}^T \bar{\mathbf{S}}_k \mathbf{B} - \mathbf{Q}^{-1} \mathbf{u}_d - \mathbf{x}_d \bar{\mathbf{S}}_k \mathbf{B})^T \mathbf{\Sigma}_k^{-1} \\ &\left. \left. (\mathbf{u}_k + (\mathbf{\Sigma}_k (\mathbf{x}_{k-1}^T \mathbf{A}^T \bar{\mathbf{S}}_k \mathbf{B} - \mathbf{Q}^{-1} \mathbf{u}_d - \mathbf{x}_d \bar{\mathbf{S}}_k \mathbf{B})) \right) \right], \end{aligned}$$

which is in fact the Gaussian in (11) with $\boldsymbol{\mu}_k^*$ and $\boldsymbol{\Sigma}_k^*$ given by (12). Note that ω_k does not appear in the backward recursion (12) since it simplifies in the calculations.

References

- Ab Azar, N., Shahmansoorian, A., Davoudi, M., 2020. From inverse optimal control to inverse reinforcement learning: A historical review. *Annual Reviews in Control* 50, 119–138.
- Ben-Tal, A., Teboulle, M., Charnes, A., 1988. The Role of Duality in Optimization Problems Involving Entropy Functionals with Applications to Information Theory. *Journal of Optimization Theory and Applications* 58, 209–223.
- Bertsekas, D., 2021. Multiagent Reinforcement Learning: Rollout and Policy Iteration. *IEEE/CAA Journal of Automatica Sinica* 8 (2), 249–272.
- Bryson, A. E., 1996. Optimal control-1950 to 1985. *IEEE Control Systems Magazine* 16, 26–33.
- Cammardella, N., Bušić, A., Ji, Y., Meyn, S., 2019. Kullback-Leibler-Quadratic Optimal Control of Flexible Power Demand. In: 2019 IEEE 58th Conference on Decision and Control. pp. 4195–4201.
- Chen, Y., Georgiou, T. T., Pavon, M., 2021. Stochastic Control Liaisons: Richard Sinkhorn Meets Gaspard Monge on a Schrödinger Bridge. *SIAM Review* 63 (2), 249–313.
- Cover, T. M., Thomas, J. A., 2006. *Elements of Information Theory* (Wiley Series in Telecommunications and Signal Processing). Wiley-Interscience, USA.
- Crisostomi, E., Ghaddar, B., Hausler, F., Naoum-Sawaya, J., Russo, G., Shorten, R. (Eds.), 2020. *Analytics for the Sharing Economy: Mathematics, Engineering and Business Perspectives*. Springer.
- Deng, H., Krstić, M., 1997. Stochastic nonlinear stabilization — ii: Inverse optimality. *Systems & Control Letters* 32 (3), 151–159.
- Diamond, S., Boyd, S., 2016. CVXPY: A Python-embedded modeling language for convex optimization. *The Journal of Machine Learning Research* 17 (1), 2909–2913.
- Do, K., 2019. Inverse optimal control of stochastic systems driven by Lévy processes. *Automatica* 107, 539–550.
- Dvijotham, K., Todorov, E., 2010. Inverse optimal control with Linearly-Solvable MDPs. In: 27th International Conference on Machine Learning. p. 335–342.
- Finn, C., Levine, S., Abbeel, P., 2016. Guided Cost Learning: Deep Inverse Optimal Control via Policy Optimization. In: 33rd International Conference on Machine Learning. Vol. 48. p. 49–58.
- Gagliardi, D., Russo, G., 2022. On a probabilistic approach to synthesize control policies from example datasets. *Automatica* 137, 110121.
- Garrabé, E., Jesawada, H., Del Vecchio, C., Russo, G., 2023. On a Probabilistic Approach for Inverse Data-Driven Optimal Control. In: 2023 62nd IEEE Conference on Decision and Control (CDC). pp. 4411–4416.
- Garrabe, E., Russo, G., 2022. Probabilistic design of optimal sequential decision-making algorithms in learning and control. *Annual Reviews in Control* 54, 81–102.

- Guan, P., Raginsky, M., Willett, R. M., 2014. On-line Markov Decision Processes with Kullback–Leibler Control Cost. *IEEE Transactions on Automatic Control* 59, 1423–1438.
- Jouini, T., Rantzer, A., 2022. On Cost Design in Applications of Optimal Control. *IEEE Control Systems Letters* 6, 452–457.
- Kalakrishnan, M., Pastor, P., Righetti, L., Schaal, S., 2013. Learning objective functions for manipulation. In: 2013 IEEE International Conference on Robotics and Automation. pp. 1331–1336.
- Karasev, V., Chiuso, A., Soatto, S., 2012. Controlled Recognition Bounds for Visual Learning and Exploration. In: Pereira, F., Burges, C., Bottou, L., Weinberger, K. (Eds.), *Advances in Neural Information Processing Systems*. Vol. 25. Curran Associates, Inc.
- Kárný, M., Guy, T. V., 2006. Fully probabilistic control design. *Systems & Control Letters* 55 (4), 259–265.
- Kullback, S., Leibler, R., 1951. On information and sufficiency. *Annals of Mathematical Statistics* 22, 79–87.
- Kárný, M., 1996. Towards fully probabilistic control design. *Automatica* 32 (12), 1719–1722.
- Levine, S., Koltun, V., 2012. Continuous Inverse Optimal Control with Locally Optimal Examples. In: 29th International Conference on Machine Learning. p. 475–482.
- Levine, S., Popovic, Z., Koltun, V., 2011. Nonlinear Inverse Reinforcement Learning with Gaussian Processes. In: *Advances in Neural Information Processing Systems*. Vol. 24.
- Lian, B., Xue, W., Lewis, F. L., Chai, T., 2022. Inverse reinforcement learning for multi-player noncooperative apprentice games. *Automatica* 145, 110524.
- Mehr, N., Wang, M., Bhatt, M., Schwager, M., 2023. Maximum-Entropy Multi-Agent Dynamic Games: Forward and Inverse Solutions. *IEEE Transactions on Robotics*, 1–15.
- Nair, S. H., Tseng, E. H., Borrelli, F., 2022. Collision Avoidance for Dynamic Obstacles with Uncertain Predictions using Model Predictive Control. In: 2022 IEEE 61st Conference on Decision and Control (CDC). pp. 5267–5272.
- Nakano, Y., 2023. Inverse stochastic optimal controls. *Automatica* 149, 110831.
- Notarnicola, I., Sun, Y., Scutari, G., Notarstefano, G., 2021. Distributed Big-Data Optimization via Blockwise Gradient Tracking. *IEEE Transactions on Automatic Control* 66 (5), 2045–2060.
- Nutz, M., 2020. Introduction to Entropic Optimal Transport. Lecture notes.
- Pegueroles, B. G., Russo, G., June 2019. On robust stability of fully probabilistic control with respect to data-driven model uncertainties. In: 2019 18th European Control Conference (ECC). pp. 2460–2465.
- Ratliff, L. J., Mazumdar, E., 2020. Inverse Risk-Sensitive Reinforcement Learning. *IEEE Transactions on Automatic Control* 65, 1256–1263.
- Rodrigues, L., 2022. Inverse Optimal Control with Discount Factor for Continuous and Discrete-Time Control-Affine Systems and Reinforcement Learning. In: 2022 IEEE 61st Conference on Decision and Control. pp. 5783–5788.
- Russo, G., 2021. On the Crowdsourcing of Behaviors for Autonomous Agents. *IEEE Control Systems Letters* 5 (4), 1321–1326.
- Self, R., Abudia, M., Mahmud, S. N., Kamalapurkar, R., 2022. Model-based inverse reinforcement learning for deterministic systems. *Automatica* 140, 110242.
- Sutton, R. S., Barto, A. G., 1998. Introduction to Reinforcement Learning, 1st Edition. MIT Press, Cambridge, MA, USA.
- Terpin, A., Lanzetti, N., Dörfler, F., 2023. Dynamic Programming in Probability Spaces via Optimal Transport.
- Todorov, E., 2009. Efficient computation of optimal actions. *Proceedings of the National Academy of Sciences* 106 (28), 11478–11483.
- Wilson, S., Glotfelter, P., Wang, L., Mayya, S., Notoomista, G., Mote, M., Egerstedt, M., 2020. The Robotarium: Globally Impactful Opportunities, Challenges, and Lessons Learned in Remote-Access, Distributed Control of Multirobot Systems. *IEEE Control Systems Magazine* 40 (1), 26–44.
- Xue, W., Kolaric, P., Fan, J., Lian, B., Chai, T., Lewis, F. L., 2022. Inverse Reinforcement Learning in Tracking Control Based on Inverse Optimal Control. *IEEE Transactions on Cybernetics* 52 (10), 10570–10581.
- Yin, M., Iannelli, A., Smith, R. S., 2023. Maximum Likelihood Estimation in Data-Driven Modeling and Control. *IEEE Transactions on Automatic Control* 68, 317–328.
- Yoo, J., Kim, H. J., Johansson, K. H., 2016. Mapless indoor localization by trajectory learning from a crowd. In: 2016 International Conference on Indoor Positioning and Indoor Navigation (IPIN). pp. 1–7.
- Yu, C., Li, Y., Fang, H., Chen, J., 2021. System identification approach for inverse optimal control of finite-horizon linear quadratic regulators. *Automatica* 129, 109636.
- Zhou, Z., Bloem, M., Bambos, N., 2018. Infinite Time Horizon Maximum Causal Entropy Inverse Reinforcement Learning. *IEEE Transactions on Automatic Control* 63 (9), 2787–2802.
- Ziebart, B. D., Maas, A., Bagnell, J. A., Dey, A. K., 2008. Maximum Entropy Inverse Reinforcement Learning. In: *Proceedings of the 23rd National Conference on Artificial Intelligence - Volume 3. AAAI’08*. AAAI Press, p. 1433–1438.